I. SUBSTRATE CHANNELING AND RELATED PROPERTIES OF THE MALATE DEHYDROGENASE-CITRATE SYNTHASE COMPLEX

II. POLYETHYLENE GLYCOL INDUCED PROTEIN ASSOCIATIONS

By

ASIT DATTA

Bachelor of Science
University of Calcutta
Calcutta, India
1974

Master of Science
University of Calcutta
Calcutta, India
1976

Submitted to the Faculty of the
Graduate College of the
Oklahoma State University
in partial fulfillment of
the requirements for
the Degree of
DOCTOR OF PHILOSOPHY
December, 1984

I. SUBSTRATE CHANNELING AND RELATED PROPERTIES OF THE MALATE DEHYDROGENASE-CITRATE SYNTHASE COMPLEX

II. POLYETHYLENE GLYCOL INDUCED PROTEIN ASSOCIATIONS

Thesis Approved:

H. Olin Spivey
Thesis Adviser

Franklin R. Leach

Roger E. Koeppe

Chenyan yu

Bruce J. Auhen

Norman N. Durham
Dean of the Graduate College

To my parents

ACKNOWLEDGEMENTS

I wish to express my sincere gratitude to my major adviser, Dr. H. Olin Spivey, for his intelligent guidance, concern, and invaluable help. I also enjoyed very much my personal relationship with him. Special thanks are due to Dr. Bruce J. Ackerson for his kind permission to use the dynamic light scattering instruments. I also thank Dr. Roger E. Koeppe, Dr. Chang-An Yu, and Dr. Franklin Leach for their valuable time spent as members of the advisory committee.

Special appreciation is extended to Dr. Jerry Merz who helped me in many ways with his versatile expertise and skill. I wish to express how much I enjoyed knowing and working with him. I am also thankful to Dr. Andrew J. Mort for his wise counsel and Julja Burchard for her technical assistance in the initial stage of my research.

I especially thank my wife, Jhuma, for the love, encouragement, and patience with which she supported me during the period and also for the immense help she provided in preparing and typing this thesis.

I dedicate this thesis to my parents, Mr. Amal Krishna Dutt and Mrs. Roma Dutt, whose inspiration and sacrifice have made the whole accomplishment possible.

TABLE OF CONTENTS

Chapter Page

PART ONE

I. INTRODUCTION 2

Enzymes in the Mitochondria 3
Enzyme Association and its Consequences . . . 4
Homologous Associations 4
Heterologous Associations 5
Catalytic and Kinetic Consequences . . . 6
Objectives and General Strategy 8
Advantages of PEG 9
Studies of the Kinetic and Catalytic Properties--Concept of Substrate Channeling 10
Summary of Rationale and Objectives 13

II. EXPERIMENTAL 15

Materials 15
Methods 15
Enzyme Preparations and Assays 15
Preparation of MDH-CS Solid-State Aggregates 16
Solubility Measurements with MC System . 17
Kinetic Measurements and Study of Solubilization 17
Lag-Time Measurements 18
Theory 18
Experimental 19
Coupled Enzyme Reaction--Substrate Channeling ("Trapping" Experiment) . . 20
Theory 20
Experimental 20

III. RESULTS AND DISCUSSION 22

Solubility Studies 22
Solubility of MDH and CS with PEG Concentration 22
Solubility vs Ionic Strength 27
Solubility vs pH 28
Kinetic Studies 41

Chapter Page

Distinguishing Dissolved from Solid-State Enzymes 42
Lag-Time Measurements 49
"Trapping" Experiment 65

IV. SUMMARY AND CONCLUSIONS 75

Solubility Profiles of MDH and CS 75
Kinetic Studies and Substrate Channeling . . 76

A SELECTED BIBLIOGRAPHY 80

PART TWO

I. INTRODUCTION 84

Rationale and Objectives 86

II. EXPERIMENTAL 89

Materials 89
Methods 90
Dynamic Light Scattering 90
Theory 90
Experimental 96

III. RESULTS AND DISCUSSION 98

IV. SUMMARY AND CONCLUSIONS 107

A SELECTED BIBLIOGRAPHY 109

LIST OF TABLES

Table — Page

PART ONE

I. Kinetic Constants of Soluble Enzymes in 34% PEG, 10°C 51

II. Lag-Time Measurement with Soluble Enzymes in 34% PEG, 10°C 54

III. Lag-Time due to DTNB Reaction 58

IV. Test for Substrate Channeling using AAT 67

V. Velocities of Reactions 70

PART TWO

I. Solubility of the Proteins in PEG Solutions . . . 99

II. Scattering Intensity of Proteins 100

III. Diffusion Coefficients in Absence of PEG 102

IV. Diffusion Coefficients and Molecular Weights in Presence of PEG 103

LIST OF FIGURES

Figure — Page

PART ONE

1. Solubility of CS in PEG 24
2. Solubility of MDH in PEG 26
3. Solubility of CS vs Ionic Strength (Phosphate Ions) 30
4. Solubility of MDH vs Ionic Strength (Phosphate Ions) 32
5. Solubility of CS vs Ionic Strength (Chloride Ions) 34
6. Solubility of MDH vs Ionic Strength (Chloride Ions) 36
7. Solubility of CS vs pH 38
8. Solubility of MDH vs pH 40
9. Effect of PEG on MDH 45
10. Time Course of Solubilization 48
11. Double Reciprocal Plot of Soluble CS 53
12. Rate Constant of DTNB Reaction 56
13. Progress Curves for MDH 60
14. Progress Curves for CS 62
15. Lag-Time Measurements with Solid-State MC Complex 64
16. V_{max} of Solid-State MDH 73

PART TWO

1. Normalized Cross-Correlation Functions 95

NOMENCLATURE

AAT	Aspartate aminotransferase
BSA	Bovine serum albumin
CoA	Coenzyme A
CoASAc	Acetyl CoA
cp	Centipoise
CS	Citrate synthase
D	Diffusion coefficient
DLS	Dynamic light scattering
DTNB	5,5'-dithiobis-(2-nitrobenzoic acid)
$g(\tau)$	Autocorrelation function
GDH	Glutamate dehydrogenase
G6PD	Glucose-6-phosphate dehydrogenase
Kd	Kilodalton
K_m	Michaelis constant
KP_i	Potassium phosphate
m(Enz)	Mitochondrial enzyme
MDH	Malate dehydrogenase
MOPS	2-(N-morpholino)propane-sulphonic acid
MW	Molecular weight
n	Refractive index
NAD	Nicotinamide adenine dinucleotide
NADH	Nicotinamide adenine dinucleotide, reduced form
nm	Nanometer

OAA	Oxaloacetate
PEG	Polyethylene glycol
U	Units
V_{max}	Maximum velocity
η	Viscosity
θ	Angle of observation
λ	Wavelength of incident light
τ	With respect to coupled reaction, lag-time With respect to light scattering, autocorrelation time

PART ONE

SUBSTRATE CHANNELING AND RELATED PROPERTIES OF THE MALATE DEHYDROGENASE-CITRATE SYNTHASE COMPLEX

CHAPTER I

INTRODUCTION

The subject of biological compartmentations has drawn the attention of scientists in their attempts to define more clearly the mechanism of metabolic processes within a cell. Different types of compartmentation can be visioned in a biological system. (a) In an individual cell, compartmentation is achieved with organelles (nuclei, mitochondria, cytoplasm, lysosomes) separated from each other by enclosing membranes. Even prokaryotic cells have the separate regions of cytosol and periplasmic space. (b) Membrane-bound and solution-phase enzymes provide another type of spatial separation of metabolic reactions. (c) Another type of compartmentation which is often overlooked is the separate "pools" of metabolic intermediates in free solution or bound to macromolecules (1). Oxaloacetate (OAA), which is an important metabolic regulator, is a significant compound in this respect. The concentration of protein-bound OAA is about three orders of magnitude higher than the free OAA concentration in the mitochondria. (d) Finally, compartmentation exists between enzymes which are functionally close to each other. Recent studies have provided increasing evidence of such specific enzyme

associations, which are described in detail in the following sections. In the case of the enzymes, their catalytic activity is governed or modified, to a large extent, by the surrounding microenvironment which, by itself, is a microcompartmentation that is helpful to understanding the reactions catalyzed by those enzymes. In this project, we have studied the properties and kinetic parameters of the complex of malate dehydrogenase (MDH) and citrate synthase (CS), which are two Krebs cycle enzymes located in the mitochondrial matrix.

Enzymes in the Mitochondria

A mitochondrion has four separate metabolic compartments--the outer membrane, the inner membrane, the intermembrane space, and the matrix space.

Mitochondrial matrix contains an unusually high concentration of proteins and current evidence (2, 3) indicates that many of these mitochondrial enzymes exist in localized solid-state aggregates. Srere (2) calculated that the enzyme molecules within the mitochondrial matrix would have to be nearly in physical contact with each other to achieve the known protein concentration of the matrix (60% protein by weight). Because of the high protein density and very little water content (4) in the protein rich phase of the matrix, it is expected that matrix proteins are unlikely to exist in true solutions.

Enzyme Association and its Consequences

The phenomenon of enzyme association can be classified under two categories: (a) homologous association and (b) heterologous association.

Homologous Associations

At cellular concentrations, several enzymes self-associate to form homologous enzyme complexes with enhanced catalytic properties. For example, erythrocyte glutamate 6-phosphate dehydrogenase (G6PD) undergoes a four-fold increase in specific activity upon association (5). Bovine liver glutamate dehydrogenase (GDH) also undergoes extensive self-association and consequent changes in its regulation by purine nucleotides. In some cases, these associations are very sensitive to the conditions of the solvents. For instance, chymotrypsin and chymotrypsinogen self-associate at low ionic strength with gradual decrease in association with increase in ionic strength. Another protein, β-lactoglobin, self-associates at pH 4.5, but not at pH 3.0 and pH 8.0.

Also the synthetic polymer, polyethylene glycol (PEG) can enhance the self-association of a wide variety of proteins below their solubility limit, which is the topic of the second part of this thesis.

Heterologous Associations

An important factor which can enhance or induce specific enzyme associations even at low concentrations of the associating enzymes is the presence of other macromolecules. This is thought to result from the entropy of excluded volume of macromolecules (6). Nonionic polymer media, like PEG, have been used to simulate such effects in vitro and generate such enzyme complexes. In this way, heterologous complexes between mitochondrial aspartate aminotransferase (mAAT) and mitochondrial MDH (mMDH) (7), MDH and GDH (8), CS and mMDH (9) have been indicated.

Fahien and Kmiotek (8) obtained extensive coprecipitation of GDH and mAAT or mMDH. If any one of these three enzymes is incubated alone or with several others at the same concentrations there is considerably less or no precipitation, indicating specificity in association among these enzymes. Palmitoyl-CoA markedly enhanced the association of GDH and MDH.

Association of a soluble mixture of AAT and MDH in presence of polymer mixture was observed by Bachmann and Johansson (7). The association was quite specific in the sense that only cytoplasmic forms of the enzymes associate with each other, as do the mitochondrial forms; but no inter-association of cytoplasmic form of one enzyme with the mitochondrial form of the other was observed.

Halper and Srere (9) succeeded in obtaining

co-precipitation of CS and mMDH in 14% PEG. Little if any of either enzyme sedimented in the absence of the other. Here also a striking specificity was observed in that no precipitation was observed when mMDH was replaced with cytosolic MDH, bovine serum albumin (BSA) or any of the other proteins tested. All these evidences suggest that metabolically adjacent enzymes associate with each other.

Catalytic and Kinetic Consequences

Organized arrays of metabolically related enzymes should provide advantages relative to a random array of enzymes. As Srere (10) pointed out, "one could imagine that a fewer number of intermediate molecules confined to a microenvironment would have a higher chemical potential than the same number of molecules in disorganized system." Experimental verifications of this hypothesis have indeed been observed, as we will see in the following paragraphs.

If two sequential metabolic enzymes are complexed together or immobilized in the vicinity of each other, then it is quite reasonable to expect a kinetic advantage if the product of the first reaction, which is the substrate of the second enzyme reaction, remains in the vicinity of its formation for a time longer than the turnover time of the second enzyme. Of course, in this context one has to consider the diffusion time of the product-substrate compared to the turnover time of the second enzyme. Srere's calculations (10) show that with the very little water

content in the mitochondrial matrix, the diffusion time of small molecules between enzymes (10^{-8} sec) is much faster than the turnover time of most enzymes (10^{-3} sec). So, the kinetic advantage of an enzyme complex mainly rests on the fact that dilution of the intermediate by diffusion from the complex need not occur as it must for undissociated enzymes randomly distributed in the matrix. Thus an increased product-substrate concentration occurs in the microenvironment of the second enzyme of a complex (11).

By an elegant experiment, Srere et al. (12) were the first to demonstrate the kinetic advantage of immobilized enzymes over free enzymes. They immobilized MDH and CS by three different methods and monitored the coupled reaction spectrophotometrically at 412 nm. In all cases the rate of the coupled reaction was much faster (up to about 100%) when the enzymes were immobilized than when they were free in solution. Even a larger rate increase of up to about 400% was found when a third enzyme, lactate dehydrogenase (LDH) and pyruvate were incorporated into the system. The LDH reaction was used to oxidize the NADH generated in the coupled reaction, to mimic the NADH dehydrogenase system in the inner mitochondrial membrane. They did not observe any change in the K_m for OAA when CS was immobilized, which could have been an alternate explanation of the increased rates. Therefore, they concluded that the locally increased concentration of oxaloacetate (OAA) in the microenvironment of CS in the immobilized enzyme system is responsible for

the increase in the rate of the reaction. The effectiveness of lowering NADH concentration in the matrix by the addition of LDH shows an additional microenvironmental effect.

Objectives and General Strategy

Though the experiments of Halper and Srere (9) indicate that MDH and CS form heterocomplexes in the solution phase, the nature and extent of this association is not known. Also the kinetic properties of the heterocomplexes are unknown. In view of the demonstrated complex formation between MDH and CS (9, 13) we decided to characterize more closely the MDH-CS complex (which we call MC complex for brevity) generated in presence of PEG and to study its catalytic properties. MDH and CS are two Krebs cycle enzymes. The reactions they catalyze are the following

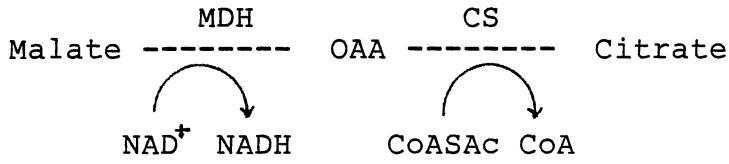

(1-1)

The molecular weight of MDH is 70,000. The enzyme consists of two identical subunits with molecular weights of 35,000 each. Eucaryotic CS has a molecular weight of 100,000 and is dissociable into two inactive physically indistinguishable subunits. Pig heart CS consists only of amino acids. It has no prosthetic group and requires no metal ions for activity.

The synthetic polymer PEG has been used to generate the

solid-state MC complex. PEG generates solid-state enzyme complexes in vitro at enzyme concentrations which can be kinetically studied. Use of PEG has several advantages which are detailed in the following paragraph.

Advantages of PEG

The exact cause of protein association and precipitation by PEG is not yet fully known. But the most popular theory, known as "excluded volume theory" (14) claims that proteins are sterically excluded from the solvent phase occupied by PEG and are thus concentrated until association or precipitation occurs. The following properties of PEG make it a good polymer to use to induce these effects on proteins.

(i) It is very potent for inducing enzyme aggregation.

(ii) It is an unbranched polymer with no ionic groups, which makes it simpler to interpret the results.

(iii) It excludes proteins from its vicinity, i.e. it does not form PEG-protein complexes in most cases.

(iv) It is highly soluble in water.

(v) It is non-denaturing.

(vi) Having an extended, random coil like conformation, PEG provides about 50-fold higher excluded volumes per weight than do proteins. Although proteins are more physiological, the protein concentrations required to approach the excluded volumes of the mitochondrial matrix and these enzyme associations appear to be too high to allow practical

experiments *in vitro*.

Studies of the Kinetic and Catalytic Properties--Concept of "Substrate Channeling"

The catalytic properties of interest are: (i) those of the individual enzyme reactions and (ii) the coupled reaction, malate to citrate. Comparisons of the properties in the solution phase with those in the solid-state were sought.

Solubility data were desired initially to: (a) choose best conditions to maintain the MC complex in the solid-state (or entirely in the solution-phase for some experiments), (b) to characterize the nature of the MDH-CS interactions. Even though it was subsequently found that kinetic measurements could not be made on the solid-state MC complex with solubility equilibrium conditions, the solubility data would permit us to find appropriate conditions for making solid-state MC complex in stock solutions used for the kinetic studies--conditions which would ensure that solid-state MC complex (a) is uncontaminated with precipitated forms of either MDH or CS, and (b) contains less than 10% of the soluble enzymes.

I have cited evidence indicating that specific enzyme associations occur predominantly between enzymes that are adjacent in the metabolic pathways. Such associations might cause altered enzyme catalytic properties. One such new property could be what has been called "substrate

channeling" between the associated enzymes. In substrate channeling, the product of first enzyme is utilized by the second enzyme prior to diffusing away from the local environment of the enzymes. Thus, such substrate molecules do not equilibrate or exchange with the bulk phase. One mechanism of substrate channeling is that used by some multienzyme complexes in which the intermediate does not dissociate from the enzyme complexes. However, functional substrate channeling may also occur to a greater or less extent even if the intermediate does dissociate from the enzyme complex. In the latter case, the enzyme concentration in the region of the enzymatically generated intermediate may be so high that the intermediate is converted to product before it has a chance to diffuse into the bulk phase. As we will describe below, this situation might be expected for an MC solid-state complex. Should this happen, it would have some physiological advantages which I discuss later. In 1970, Gaertner et al. (15) predicted the possibility of substrate channeling in a set of sequential reactions catalyzed by multienzyme complexes in Neurospora crassa. The possibility of substrate channeling in the Krebs cycle enzyme complexes has been proposed by many workers (12, 16), but to date no direct evidence has been reported. More recently, Sumegi et al. (17) and Porpaczy et al. (18) have studied the complex formations between CS and pyruvate dehydrogenase complex and also between the α-ketoglutarate dehydrogenase complex and

succinate thiokinase. They predict the possibility of substrate channeling between these enzyme complexes, but present no direct evidence for it. So, a primary objective of our studies was to establish the phenomenon of substrate channeling in our solid-state MC system. In our case the intermediate to be channeled is OAA. The concentration of OAA is considered by some to be primarily responsible for regulation of the rate of oxidation in the Krebs cycle (19). This view has been supported in recent reports also (20, 21). The apparent free concentration of OAA in the mitochondrial matrix is in dispute, but most authors consider it to be very low, about 40 nM (22). This figure is so low that the rate of its reaction catalyzed by CS is not commensurate with the known rate of the cycle in the mitochondria, estimated from oxygen utilization. The channeling of OAA between MDH and CS has the merit of resolving this controversy.

So lack of direct experimental evidence and the necessity of resolving the important issue of rate and regulation of Krebs cycle inspired us to direct our efforts towards investigating the phenomenon of substrate channeling in the soild-state MC complex. If the occurrence of OAA channeling between MDH and CS prove to be true, it would not only broaden our understanding on the mechanism of action of multienzyme complexes, but also shed light on the efficiency and regulatory mechanism of Krebs cycle.

Summary of Rationale and Objectives

Current evidence indicates that many of the enzymes of the mitochondrial matrix exist in localized solid-state aggregates. Most of these enzymes exist in the cells at concentrations 1000-fold or more higher than can be used for most kinetic studies *in vitro* utilizing conventional kinetic methods. I also cited evidence indicating that specific enzyme associations would occur predominantly between enzymes that are adjacent in metabolic pathways. Such associations would likely cause altered enzyme catalytic properties. All these facts stress the importance of studying the properties of solid-state enzyme complex in greater detail to understand the mechanism of action of these enzyme complexes and the regulatory mechanism of the metabolic pathways more clearly. We chose to investigate the solid-state complex of MDH and CS. Addition of PEG to enzyme solutions is a tool to generate such solid-state enzyme complexes *in vitro* at enzyme concentrations which can be studied. If the majority of MDH and CS is physically complexed with each other in the mitochondrial matrix, it is possible that OAA generated by MDH will be converted to citrate locally and never equlibrate with the matrix volume outside of this enzyme complex. This localization of an enzymatically generated intermediate in the space occupied by the next enzyme is termed "substrate channeling". Our ultimate goal is to investigate if there is any substrate

channeling in our *in vitro* system. In pursuit of this goal, we first attempt to characterize the solubilities of our MC complex under different solution conditions and subsequently to study the kinetic properties of the solid-state and soluble MC complex.

CHAPTER II

EXPERIMENTAL

Materials

Ammonium sulfate suspensions of enzymes were from Sigma Chemical Corporation as follows: CS (Type III), mMDH and AAT (Type I). Coenzyme A, malic acid, NADH (Grade III), NAD^+ (Grade III), OAA and 5,5'-dithiobis - (2-nitrobenzoic acid) (DTNB) were also from Sigma. Glutamic acid was from Calbiochem and polyethylene glycol (PEG 6000) was from Matheson Coleman and Bell. PEG solutions were made in 10 mM potassium phosphate buffer and the pH adjusted to 7.5.

Methods

Enzyme Preparations and Assays

CS and MDH were desalted by centrifugally eluting the enzymes through G-50 Sephadex columns (23). The enzymes were diluted in 10 mM potassium phosphate buffer, pH 7.5 and protein concentrations were determined by measuring absorbance at 280 nm. Specific absorptivities of 1.78 and 0.250 $(mg/ml)^{-1}cm^{-1}$ were used for the synthase (24) and dehydrogenase (25), respectively. All enzymes were routinely assayed at room temperature in a 1 cm path length

cell. CS was assayed (26) using 0.1 mM acetyl-CoA (CoASAc), 0.5 mM OAA, 0.4 mM DTNB and 100 mM potassium phosphate buffer (pH 7.5) and 412 nm light. CoASAc was made by acetylation of CoA with acetic anhydride. MDH was assayed (27) using 0.2 mM NADH, 0.05 mM OAA and 100 mM potassium phosphate buffer (pH 7.5) with 340 nm light. AAT was assayed (28) with 0.5 mM OAA, 20 mM glutamate and 100 mM potassium phosphate buffer (pH 7.5) using OAA absorption at 280 nm. Absorptivity changes assumed were 13600, 6220, and 528 $M^{-1}cm^{-1}$ for the DTNB (26), NADH and OAA (28) reactions, respectively. Specific activities of enzymes were approximately 120 U/mg, 500 U/mg, and 100 U/mg for the synthase, dehydrogenase and transferase respectively.

Preparation of MDH-CS Solid-State Aggregates

MDH and CS were incubated with 10% PEG (w/v) at 10°C for approximately an hour at concentrations below their individual solubility limit. In a typical preparation, we used 2 mg/ml of each of the enzymes. The turbid homogenate was centrifuged at 10,000g for 40 minutes at 10°C to get a pellet containing 90% of both enzyme activities. Negligible enzyme activities were found in the supernatant. The pellet was then suspended in 30% PEG with the aid of a plumper until a homogeneous turbid suspension of solid-state enzyme aggregate was obtained. This suspension was the stock source of MC complex used for solubility, association or

kinetic studies. Enzyme quantities in the aggregates were determined by enzyme activity measurements on aliquots of dissolved suspensions. We observed a ratio of 3 mol CS / 2 mol MDH in the suspension. The aggregates, thus formed, were stored at 0-4^{o}C. The enzymes were found to be quite stable for at least a few weeks in the presence of 30% PEG.

Solubility Measurements with MC System

Solubility measurements were made by transferring a suspension of stock MC to solution with different PEG concentrations at different ionic strengths and pH values. Enzyme contents in the pellets and in the supernatants at different conditions were determined by enzyme activity measurements after centrifugation at 10,000g for 40 minutes. The ionic strengths were calculated using a computer program BUFFER written in this laboratory, which calculates the pH and ionic strength of dilute phosphate buffers made from concentrated buffers. Direct measurements of pH on the dilute buffers were found very unreliable with the commonly available electrodes (29). This problem has become more severe in recent years with electrodes made with slower flowing liquid junctions.

Kinetic Measurements and Study of Solubilization

A small aliquot of a solid-state suspension of enzymes (MC, MDH, or CS) was transferred from a stock solution to

the reaction cuvette containing 34% (w/v) PEG. Specific activities were measured before the solid-state suspension dissolves. The difference between specific activities of solution- and solid-phase enzymes were used to monitor the rate of solubilization of the solid-phase enzyme complex. Kinetic constants of the enzymes were determined in the usual way by varying the substrate concentrations and plotting Lineweaver-Burk plots or by progress curve analysis using the least square analysis program CRICF (30).

Lag time and "trapping" experiments with AAT were separate strategies employed to reveal substrate channeling. For reasons discussed in the following chapter, the latter strategy was considered preferable, especially in our system.

Lag-Time Measurements

Theory. In a coupled sequential enzymatic reaction where the product of the first reaction is the substrate of the second reaction, the lag-time is defined as the time taken by the intermediate (which is OAA in our case) to reach a steady-state concentration. Graphically this behaviour can be observed as a lag-transient before the rate of product formation reaches a steady-state velocity. Quantitatively, the formation of the second product in the coupled sequential reaction is governed by the following equation (31)

$$P = vt + v(e^{-kt}-1)/k \qquad (2\text{-}1)$$

as long as the velocity, v, of the first reaction is constant and the concentration of the intermediate is low enough for the second reaction to be first order with respect to the intermediate. The rate constant $k = V_2/K_2$ where K_2 and V_2 are respectively the Michaelis constant and maximal velocity of the second enzyme. At the lag-time, $\tau = 1/k$, the observed reaction velocity is $(1 - e^{-1})v$. Summarizing, we have

$$\tau = 1/k = K_2/V_2 \qquad (2\text{-}2)$$

which predicts the lag-time of coupled enzyme reactions from the rate constants of the second enzyme. The final slope of the product-time curve will be equal to v, the velocity of the first reaction in Eq. (1-1).

Experimental. The coupled reactions (1-1) were measured in 34% PEG at 10°C and the production of CoA was monitored at 412 nm, by coupling it to DTNB. Nitrogen was passed through the cell holder to prevent fogging of optical windows. The reaction mixture contained 40 mM malate, 4 mM NAD^+, 0.1 mM CoASAc, 0.4 mM DTNB, 34% PEG, 100 mM potassium phosphate buffer (pH 7.5). The kinetic constants, V_2 and K_2, of the second reaction were determined under the same conditions in a separate experiment to determine the predicted lag-time.

Coupled Enzyme Reaction--Substrate Channeling ("Trapping"Experiment)

Theory. To provide a more precise test of substrate channeling, we devised a method utilizing a third enzyme to trap any intermediate escaping into the bulk phase. The enzyme we chose to use was AAT. The reaction it catalyzes is the following

$$\text{OAA} + \text{Glutamate} \xrightarrow{\text{AAT}} \text{Aspartate} + \alpha\text{-ketoglutarate}$$

So the rationale of this experiment was to trap the bulk phase OAA by AAT.

Experimental. Reactions were measured at 10°C and the production of CoA was monitored at 412 nm. Nitrogen was passed through the cell holder to prevent fogging of optical windows of the spectrophotometer. The reaction mixture contained 40 mM malate, 4 mM NAD^+, 0.1 mM CoASAc, 4 mM glutamate, 0.4 mM DTNB, 34% PEG, 100 mM potassium phosphate buffer (pH 7.5), solid-state enzyme aggregates containing CS at 2 µg/ml of assay solution, and when present, soluble AAT at a concentration of 0.2 mg/ml. Control contained everything except the AAT. The AAt was found to be sufficient to reduce the reaction with the soluble enzyme system to about 1% with comparable MDH and CS concentrations. Concentrated stock solutions of substrates were made in 100 mM potassium phosphate buffer and the pH

adjusted to 7.5 with KOH when necessary. To circumvent the problem of solubilization of the enzyme aggregats with time, yet achieve a thorough mixing in the highly viscous PEG solutions Dr. Jerry Merz contructed a special stirring device. It consisted of a small D.C. motor attached to a helical stirring rod to enhance vertical flow in the cuvette. The rod was made of Plexiglass^{TM} which had a length of 4 cm and a width of 0.5 cm. A simple control circuit was constructed to maintain the motor speed independent of the load, but continuously adjustable by the user. The apparatus was positioned above the cuvette holder of the spectrophotometer. The motor was fixed to the holder while the stirring rod dipped into the test solution in the cuvette. The adequacy of mixing by this apparatus was tested in separate pilot measurements. The criterion was the amount of time it took an enzyme reaction solution to reach a steady state velocity while being mixed in PEG solutions at 10^{o}C. We also tested mixing of dye in PEG solutions to ascertain it visibly. In most measurements, a steady state was reached within 5 seconds.

CHAPTER III

RESULTS AND DISCUSSION

Solubility Studies

Solubility of MDH and CS with PEG Concentration

We measured the solubility of MDH and CS over a range of PEG concentrations and the results have been shown in Figures 1 and 2. We incubated the enzymes, alone or together, in different PEG concentrations, in 10 mM potassium phosphate buffer (pH 7.5) at 10^{o}C. Our objective was to find a PEG concentration at which we would be able to generate a hetero-complex of the enzymes, with no homo-precipitation at all. So we had to restrict ourselves within a narrow range of PEG concentration; because at concentration lower than 9.5% the solubility was quite high, and there was no detectable enzyme association, whereas at 10.5% CS alone started to precipitate. It appears that there is a narrow window between individual enzyme precipitation and hetero-association under these conditions. Our results show that the solubility of the enzyme complex decreases rather sharply with increasing PEG concentrations, although the solubility profile of each individual enzyme is

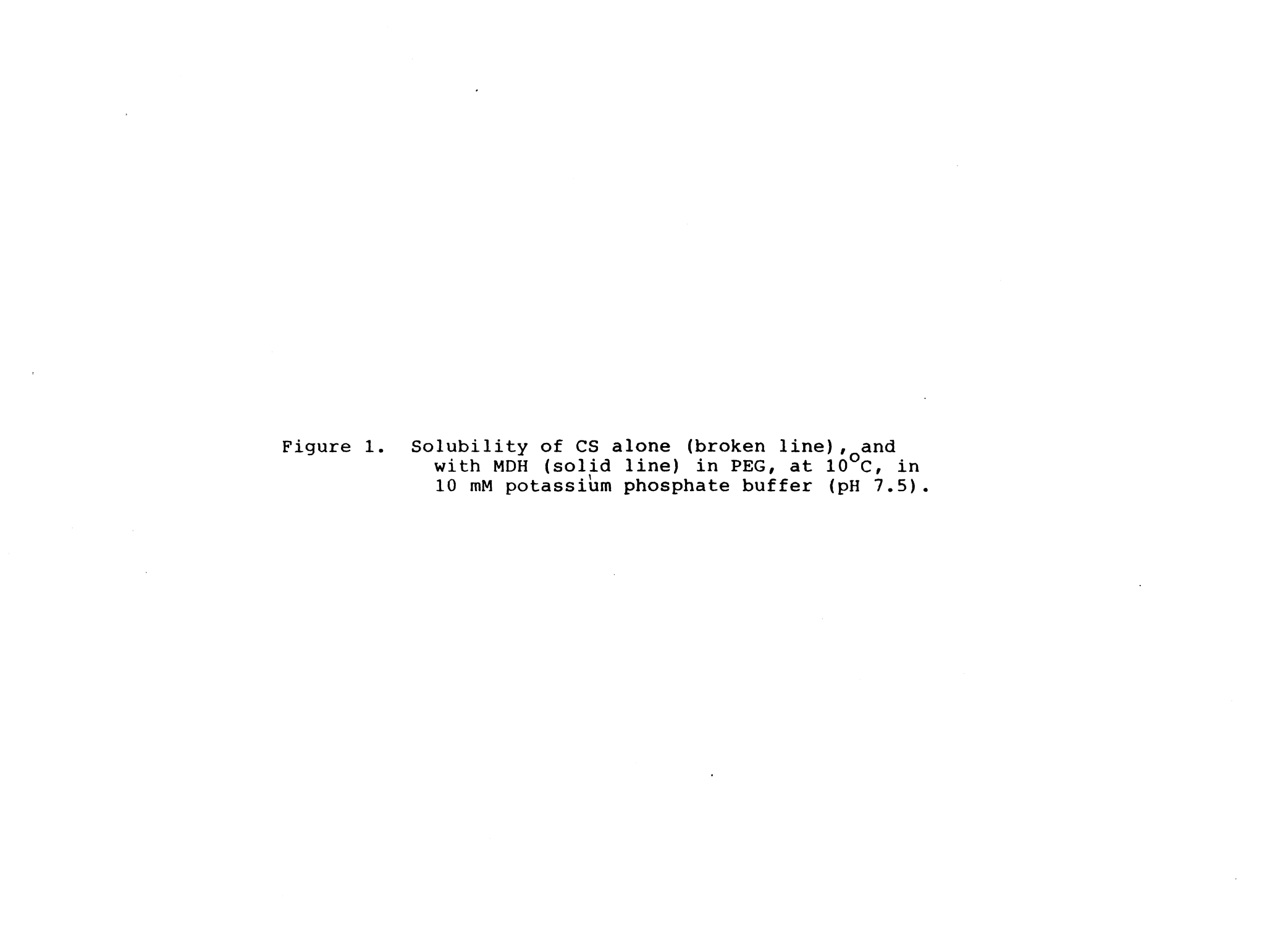

Figure 1. Solubility of CS alone (broken line), and with MDH (solid line) in PEG, at 10°C, in 10 mM potassium phosphate buffer (pH 7.5).

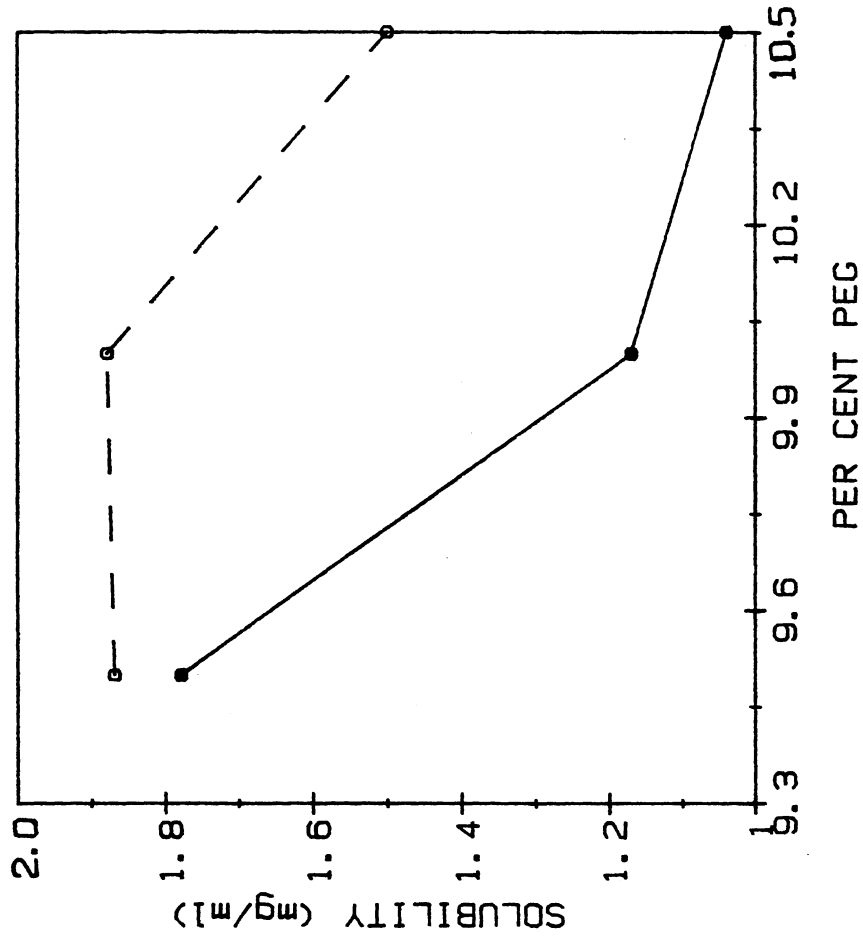
SOLUBILITY (mg/ml)
2.0
1.8
1.6
1.4
1.2
1
9.3
9.6
9.9
10.2
10.5
PER CENT PEG

Figure 2. Solubility of MDH alone (broken line), and with CS (solid line) in PEG, at 10°C, in 10 mM potassium phosphate buffer (pH 7.5).

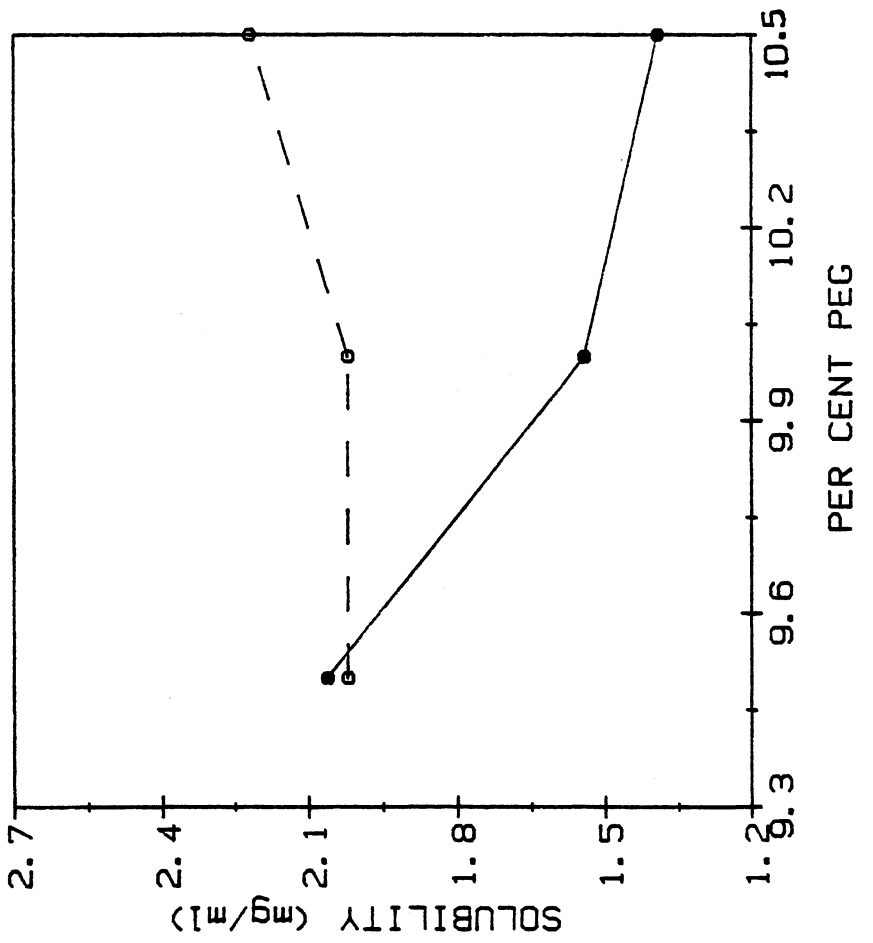
SOLUBILITY (mg/ml)
2.7
2.4
2.1
1.8
1.5
1.2
9.3
9.6
9.9
10.2
10.5
PER CENT PEG

less sharp.

In measuring the solubility of each individual enzyme and of the enzyme complex, we adopted the method of centrifugation. In this method, after incubating the enzymes we centrifuged them at a high centrifugal force (about 10,000g) to get a hard pellet. Then we measured the enzyme concentrations both in the supernatant and in the pellet by enzyme activity measurements. Solubility measurements by filtration methods were too unreliable due to enzyme losses from absorption to and denaturation by the various filters we tried. Equilibration of the filters with PEG and protein solutions prior to filtering reduced these problems, but not to the extent desired. In 10 mM phosphate buffer (pH 7.5) we got a ratio of CS to MDH of about 2 to 1 in the precipitate, which corresponds to a molar ratio of 3 to 2. This ratio might not be exact because of some experimental difficulties in determining the stoichiometry. Experiments are in progress in our laboratory to determine the stoichiometry accurately, but this does not affect our subsequent conclusions concerning substrate channeling.

Solubility vs Ionic Strength

At 10% PEG and 10 mM potassium phosphate buffer (pH 7.5) and with each enzyme at a concentration of 2 mg/ml, we were able to obtain a repeatable formation of solid-state MC aggregates without precipitating the enzymes alone. Then we decided to study the effect of ionic strength on the

solubility of the enzymes. Our data (Figures 3 and 4) show that the solubility of the MC complex increases with increase in ionic strength of the medium, although the solubility of the enzymes alone did not vary markedly over the range studied. The increase in solubility is sometimes attributed to a decrease in the size of the random coiled PEG molecules in the higher ionic strength solutions. This effect could also be due to the "salting in" observed for proteins as the ionic strength is increased from very low levels to moderate ones.

To test whether ionic strength effects were general- or specific-ion effects, the ionic strength was also increased with KCl instead of phosphate. Our results with KCl (Figures 5 and 6) show no marked differences from those with phosphate ions. Thus, it appears that the solubility of the enzymes vary in a quite general way with the ionic strength of the medium. The apparent minimum solubility of CS near 25 mM KCl may be a coincidence of experimental error, rather than real. The curves tell us that in low ionic strength solutions the solubility of one enzyme decreases in the presence of the other.

Solubility vs pH

The results of our studies on solubility of the enzymes with pH are shown in Figures 7 and 8. The general trend is that there is an increased solubility of both the enzymes with an increase in pH.

Figure 3. Solubility of CS alone (broken line), and with MDH (solid line) versus ionic strength (phosphate ions) in 10% PEG, at 10 °C.

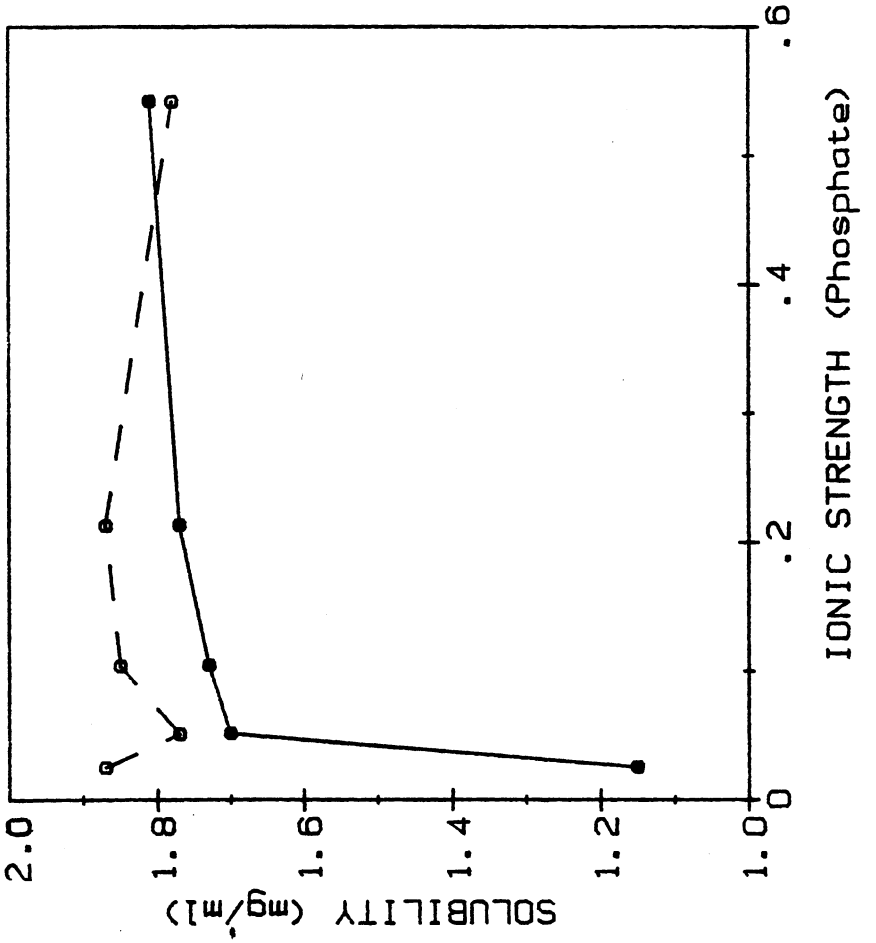
SOLUBILITY (mg/ml)
2.0
1.8
1.6
1.4
1.2
1.0
0
.2
.4
.6
IONIC STRENGTH (Phosphate)

Figure 4. Solubility of MDH alone (broken line), and with CS (solid line) versus ionic strength (phosphate ions) in 10% PEG at 10°C.

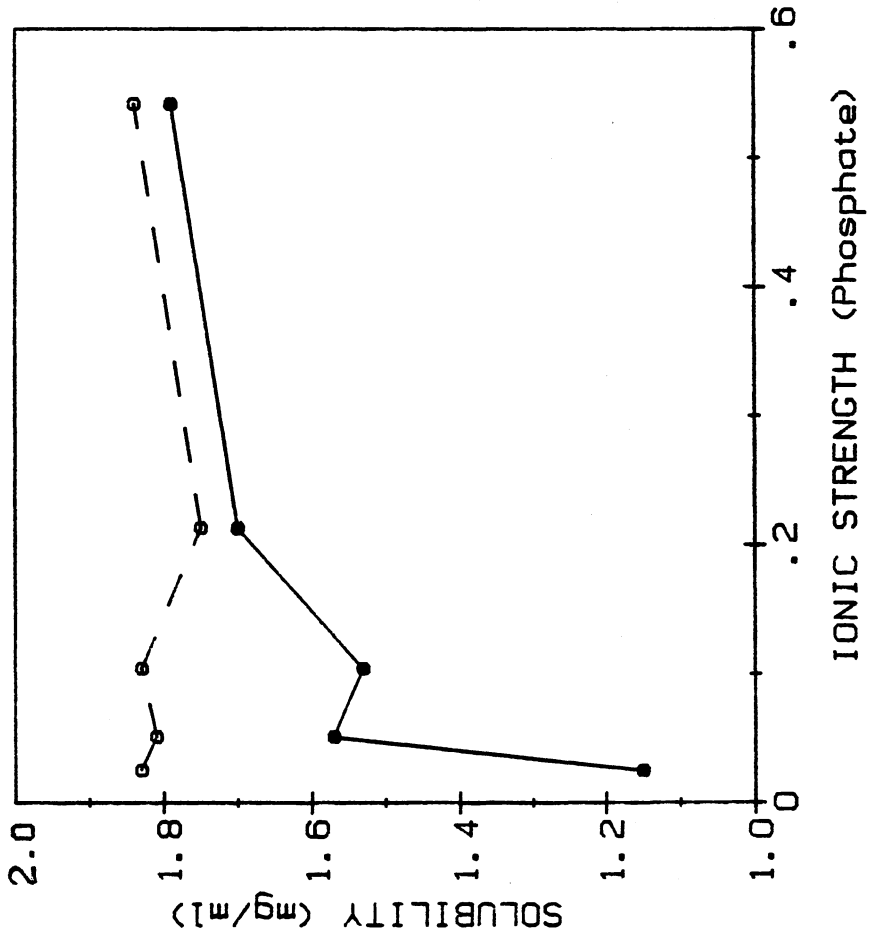
SOLUBILITY (mg/ml)
2.0
1.8
1.6
1.4
1.2
1.0
0
.2
.4
.6
IONIC STRENGTH (Phosphate)

Figure 5. Solubility of CS alone (broken line), and with MDH (solid line) versus ionic strength (chloride ions) in 10% PEG at 10°C.

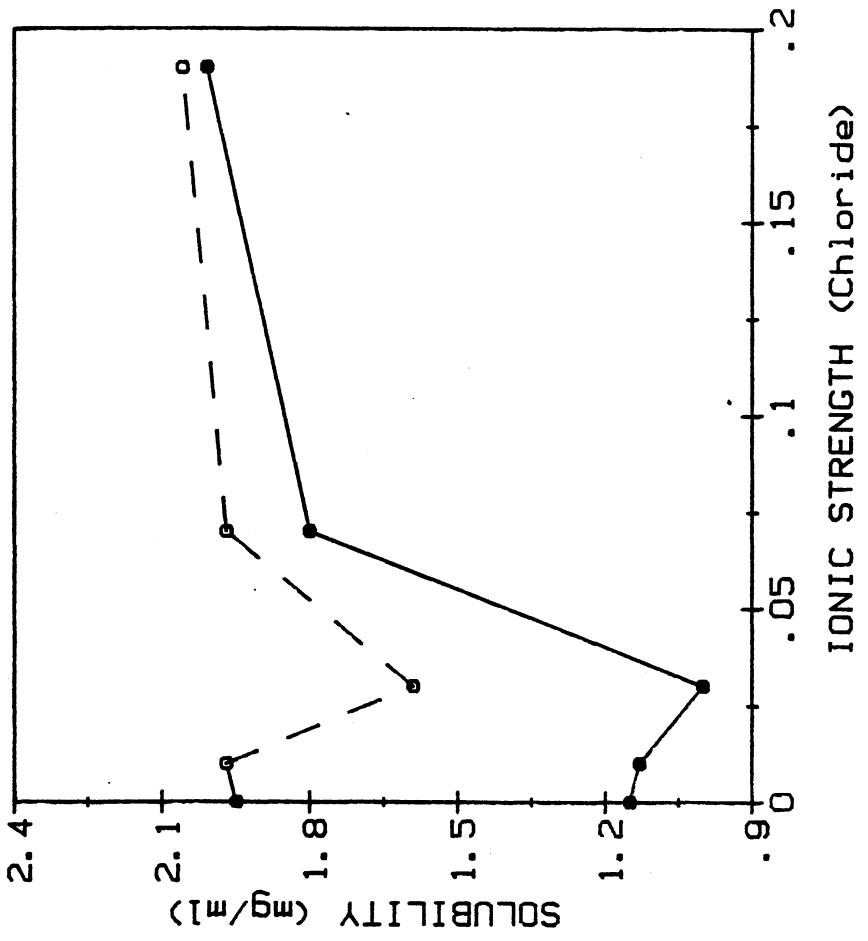
SOLUBILITY (mg/ml)
2.4
2.1
1.8
1.5
1.2
.9
0
.05
.1
.15
.2
IONIC STRENGTH (Chloride)

Figure 6. Solubility of MDH alone (broken line), and with CS (solid line) versus ionic strength (chloride ions) in 10% PEG at 10°C.

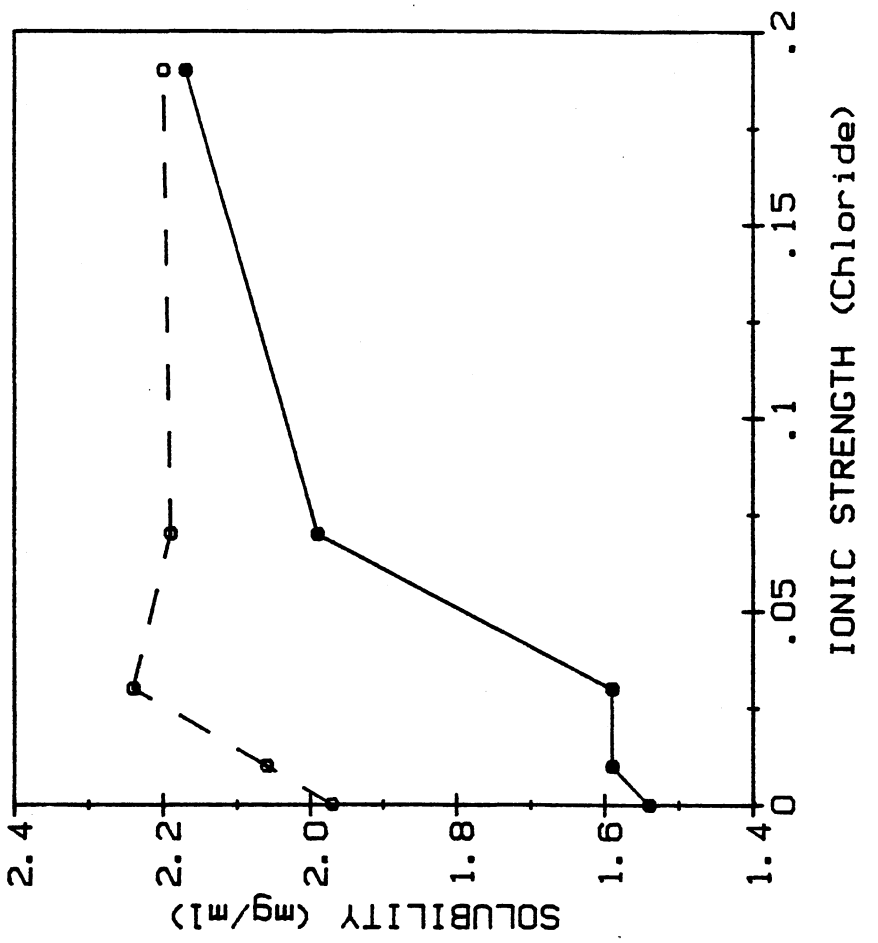
SOLUBILITY (mg/ml)
2.4
2.2
2.0
1.8
1.6
1.4
0
.05
.1
.15
.2
IONIC STRENGTH (Chloride)

Figure 7. Solubility of CS alone (broken line), and with MDH (solid line) versus pH at constant ionic strength in 10% PEG at 10°C.

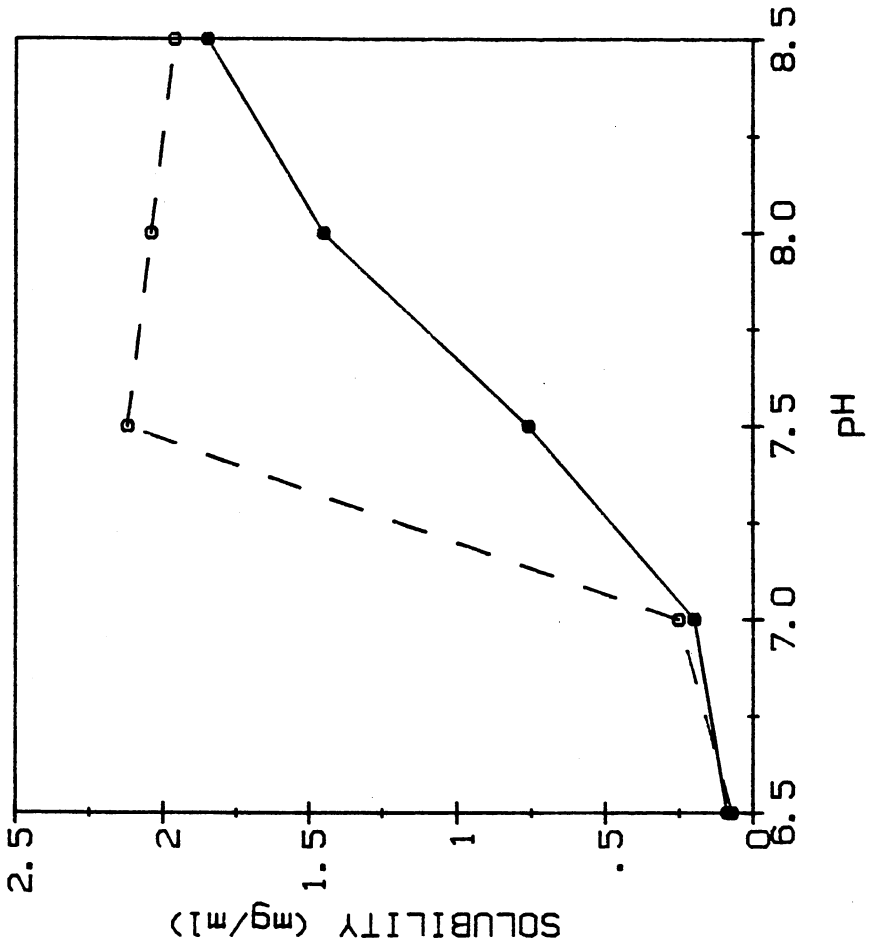
SOLUBILITY (mg/ml)
2.5
2
1.5
1
.5
0
6.5
7.0
7.5
8.0
8.5
pH

Figure 8. Solubility of MDH alone (broken line), and with CS (solid line) versus pH at constant ionic strength in 10% PEG at 10°C.

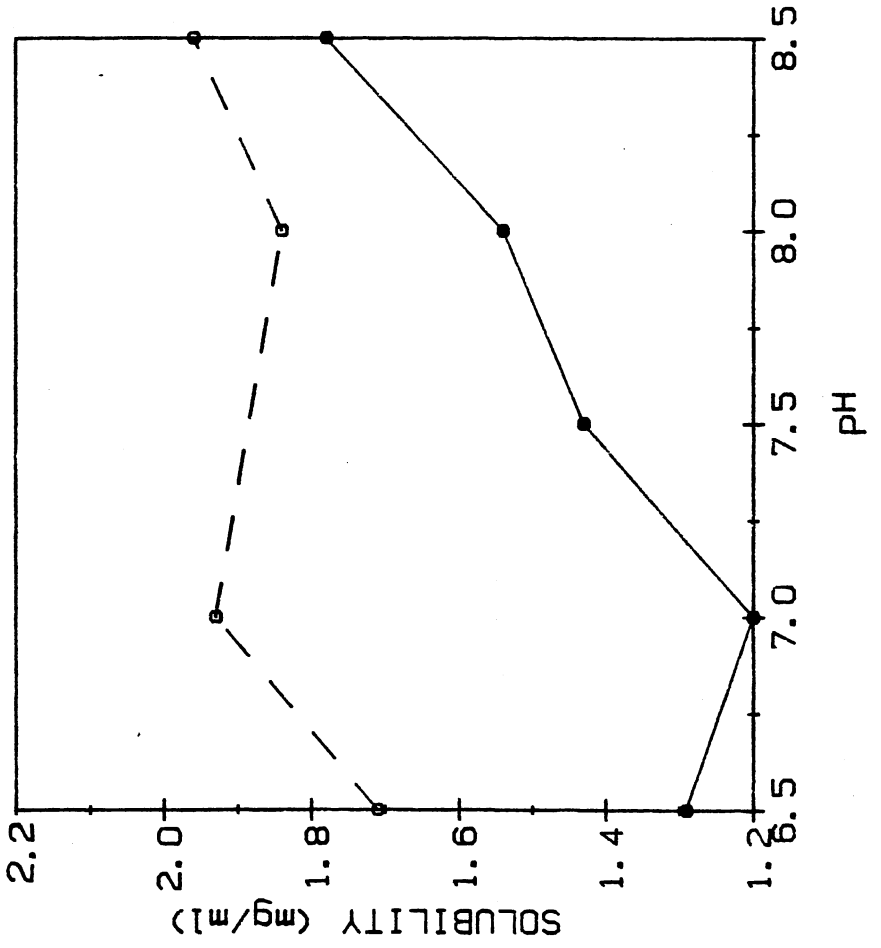
SOLUBILITY (mg/ml)
2.2
2.0
1.8
1.6
1.4
1.2
6.5
7.0
7.5
8.0
8.5
pH

We repeated some of the solubility measurements with recrystallized PEG, but the results did not vary significantly.

Kinetic Studies

The catalytic properties of the individual enzymes in the solid-state are of interest in themselves. The activity of each enzyme in the solid-state has been measured both from precepitates of the individual enzyme and from the uncoupled reaction within the solid-state MC complex. The K_m and V_m of CS within the MC complex are also needed to apply the lag-time test of substrate channeling to the MC complex. In this test, the lag-time of the solid-state enzyme complex is calculated by Eq. (2-2) using the measured kinetic parameters of the second enzyme. This calculated lag-time is then compared with the lag-time experimentally found for the coupled reactions:

$$\text{Malate} + \text{NAD}^+ + \text{CoASAc} \dashrightarrow \text{Citrate} + \text{NADH} + \text{CoA} + \text{H}^+$$

If the observed lag-time is found to be much shorter than the predicted one, this indicates that the intermediate is directly channeled (at least to a considerable extent) from the first enzyme to the second without being distributed uniformly throughout the bulk volume. Zero lag-time implies 100% substrate channeling.

Distinguishing Dissolved from Solid-State Enzymes

To characterize the solid-state enzyme complex, conditions with which the enzymes were predominantly (e.g. greater than 95%) in the solid-state were desired. Otherwise kinetic properties of solution-phase enzymes would be superimposed on those of the solid-state enzymes. Such a condition at solubility equilibrium required PEG concentrations in excess of 30% and high enzyme concentrations. The high enzyme concentrations required fast mixing methods for kinetic measurements, but extensive attempts with both continuous (32) and stopped-flow methods were unsuccessful due to the extremely high solution viscosities.

To circumvent these problems, solubility equilibrium was not used in the final assay solution, though it was achieved in the stock suspension of solid-state enzyme complex. An aliquot of the stock enzyme suspensions was transferred to the assay solution and kinetic measurements made before the solid-state enzymes dissolved. Application of this method requires a method to determine that the enzymes remain in the solid-state during the approximately 1-2 min of kinetic measurements. The conventional methods of centrifugation or filtration were unsuccessful. The high solution viscosity prevented reliable centrifugation measurements and made filtration slow. In addition,

extensive enzyme absorption and inactivation on the filters made this method unreliable. Therefore, the differences in enzyme activities between solution- and solid-phase enzymes were used to demonstrate that the enzymes remain in the solid-phase during measurements.

Figure 9 shows the effect of PEG concentration on the specific activity of MDH in MC complex. The reaction (OAA reduction) was measured either immediately after addition of enzyme complex to the assay solution (lower curve) or the enzyme complex was incubated 5 min in the assay solution with NADH prior to starting the MDH reaction by addition of OAA (upper curve). The change in the apparent specific activity with preincubation can be ascribed to the solubilization of the enzymes. Thus, Figure 9 illustrates the differences in apparent specific activities of MDH between the solution- and solid-phase states over a range of PEG concentrations. Incubation for 5 min of the solid-state MC complex before starting the reaction (upper curve) leads to solubilization of some or all of the solid-state enzymes and a higher specific activity of MDH. The rather constant specific activity of the solid curve indicates that with no incubation, the MC enzymes remains in the solid-state phase. With no preincubation, the specific activity averaged to 2.4 U/mg over the range of PEG concentrations. After the 5 min preincubation period, the specific activity increased with decreasing PEG concentration. The activity was too rapid to measure below 31% PEG. There was no difference in specific

Figure 9. Effect of PEG conc. on MDH (MC) specific activity with (broken line) and without (solid line) a 5 min preincubation period at 10°C. MDH conc. was 4 µg/ml. Standard assay solutions were used.

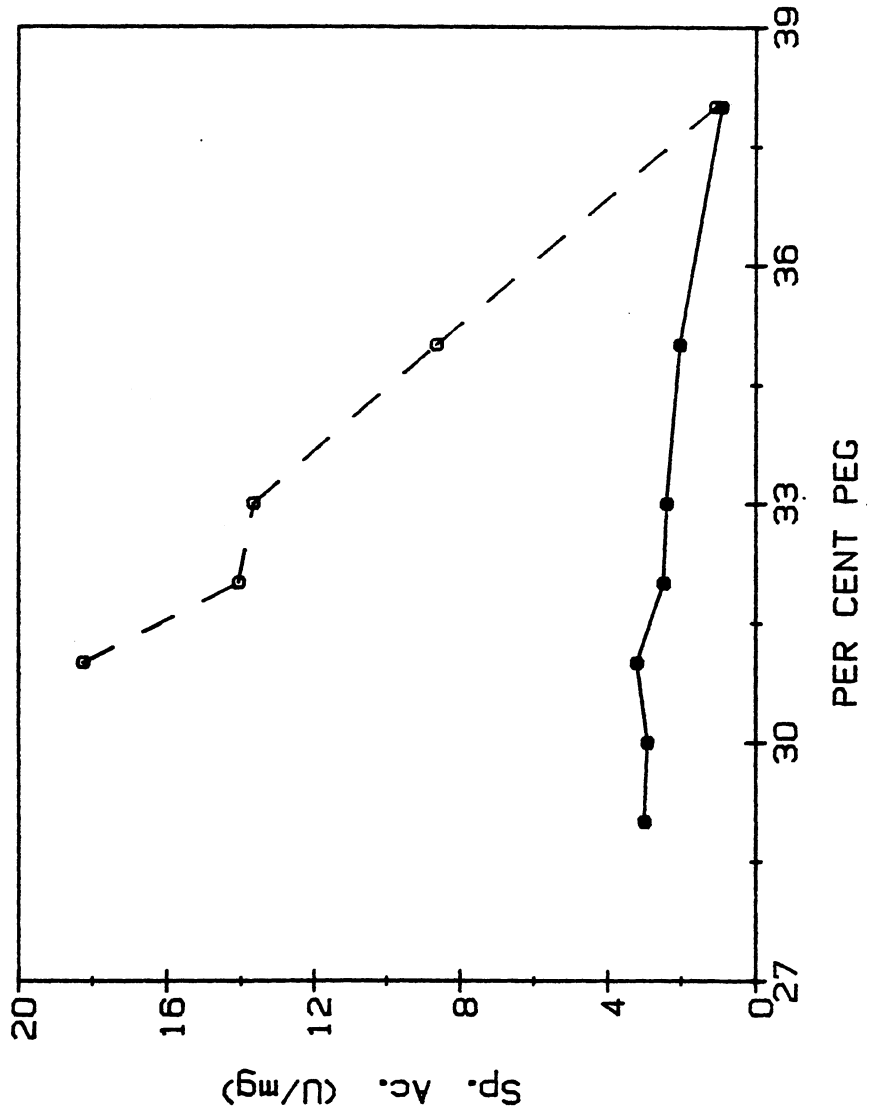
Sp. Ac. (U/mg)
20
16
12
8
4
0
27
30
33
36
39
PER CENT PEG

activity over this incubation period at 38% PEG. Similar results were found when CS activity was measured. High PEG concentrations are needed to slow rates of dissolution of the solid-state enzymes, yet too high a PEG concentration would abolish activity differences between solid- and solution-states of the enzymes. Thus a concentration of 34% PEG was chosen for subsequent measurements since the significant difference in specific activities of solution- and solid-phase enzymes at that PEG concentration could be used to monitor the solubilization of the MC aggregates. In a later measurement (data not shown) the MDH concentration was varied from 0.1 μg/ml to 4.0 μg/ml in 34% PEG with a preincubation of 10 min and specific activity was measured. The specific activity was independent of enzyme concentrations indicating that the enzyme was in a single phase rather than separated into two phases with different specific activities. Since the average specific activity, 11.1 U/mg, is close to that of the solution phase, we conclude that the upper curve corresponds to completely dissolved enzyme. Thus, we consider the decrease in specific activity with increased PEG shown in the upper curve of Figure 9 to result from PEG inhibition of MDH rather than precipitation of the enzyme.

Next we sought to assay the rate at which solubilization occurred. The specific activity of MDH was measured as a function of time. The enzymes were added as a solid-state suspension. Figure 10 indicates that the

Figure 10. Time course of solubilization. The specific activity of solid-state (solid line) and soluble (broken line) MDH (MC) versus time of incubation in 34% PEG at 10°C. The solid-state MDH conc. was 4 µg/ml and soluble MDH conc. was 0.75 µg/ml. Standard assay solutions were used.

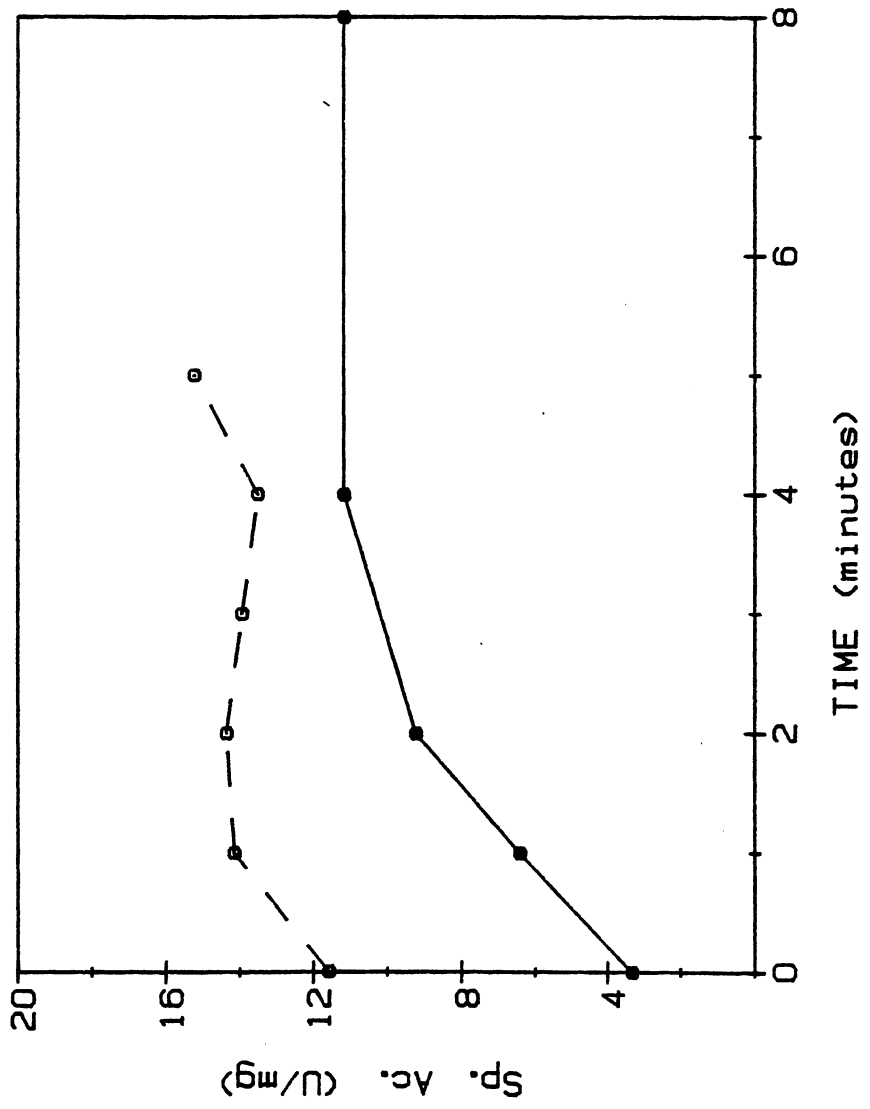
Sp. Ac. (U/mg)
20
16
12
8
4
0
2
4
6
8
TIME (minutes)

enzymes remained in the solid-state if the reaction was initiated with no preincubation, but dissolved completely within 5 minutes of preincubation (solid curve). This is consistent with our previous finding that MDH goes into solution within 10 min. Complete solubilization of the solid-state enzyme is indicated by the increase in the specific activity after 5 min which approached that of the solution phase enzyme (broken curve). In the latter case we dissolved the enzyme suspension in 10 mM potassium phosphate buffer (pH 7.5) and added that to the reaction cuvette to ensure that we are dealing with completely soluble enzymes. Calculation of specific activity, taking into account the PEG inhibition and the temperature effect, and also extrapolation of our previous light scattering data ensured us that the enzymes of the upper curve of Figure 10 were in the soluble phase over the time of measurements. In all cases we measured the slope of the reaction curve within the first minute after the reaction started during which the enzyme remains in the soluble form.

Lag-Time Measurements

Knowing the conditions for achieving the solid-state or soluble enzymes in 34% PEG, measurements of substrate channeling in the solid-state MC complex could proceed. The first strategy used was to measure lag-time, as defined under the "Methods" section in Chapter II.

The experimental values of V_2 and K_{OAA} of soluble CS in

34% PEG are given in Table I. Non-linear least square fit, which takes into account the weighting factor of each data point, was used to fit the data. Figure 11 shows the fitted curve. The predicted lag-time for the coupled reaction system is calculated by Eq. (2-2). The final rate of the coupled reaction is generally governed by V_1. The measured lag-times (Table II) of the coupled but soluble system in 34% PEG expermentally was determined by supplying substrates malate, NAD^+ and CoASAc, but no OAA, to soluble enzymes.

Our results show good agreement between predicted and observed lag-times. The experimental value, v_{max}^{obs} is, however, less than the predicted value V_1. The model equation (2-2) assumes V_2/V_1 greater than 5, with which v_{meas} approaches V_1. Computer simulations in our laboratory have shown, however, that the predicted lag-time differs very little from the experimental lag-time even when the activity of the second enzyme is considerably less than that of the first (e.g. even with $V_2/V_1 = 1/5$). Therefore, v_{max}^{obs} need not equal V_1. The lag-time quoted in Table II, however includes the intrinsic lag-time of the DTNB reaction. In a separate experiment, the lag-times of this chromophoric reaction were assessed at different DTNB concentrations (Figure 12). High enough DTNB concentration was used in the coupled reaction to represent the synthase reaction and the lag-time of the DTNB reaction was found to be approximately 1 min. It might be mentioned here that the reaction between DTNB and CoA-SH is very complex and the plot of Figure 11

TABLE I

KINETIC CONSTANTS OF SOLUBLE ENZYMES
IN 34% PEG, 10° C

Const.	CS[a]	MDH[b]
V_1	--	(0.86 ± 0.2) μM/min
V_2	(0.5 ± 0.2) μM/min	--
K_{OAA}	(12 ± 2) μM	--

[a] CS = 0.1 μg/ml.

[b] MDH = 0.5 μg/ml.

Figure 11. Double reciprocal plot of soluble CS in 34% PEG at 10°C. The data have been fitted to a non-linear least square analysis which takes into account the weighting factor of each data point.

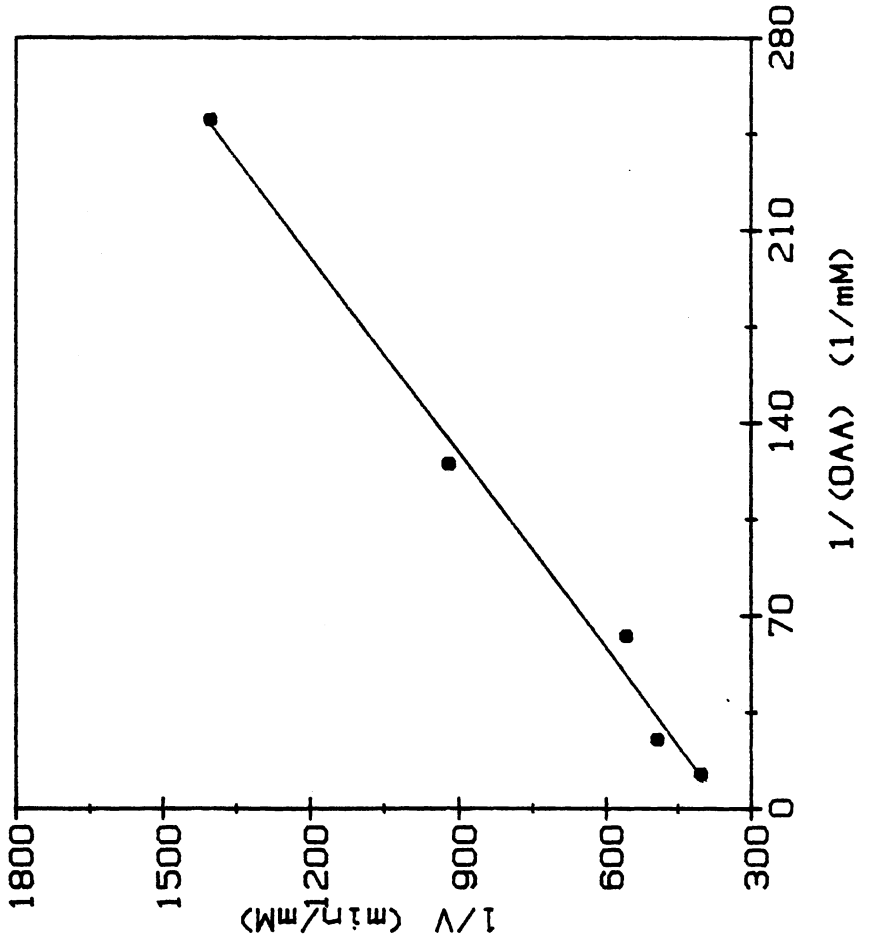
1800
1500
1200
900
600
300
1/V (min/mM)
0
70
140
210
280
1/(OAA) (1/mM)

TABLE II

LAG TIME MEASUREMENT WITH SOLUBLE ENZYMES IN 34% PEG, 10° C

Run	V_1^{pred} μM/min	v_{max}^{obs} μM/min	τ^{calc} min	τ^{obs} min
1[a]	0.86	0.16	4.8	4.7
2[b]	0.43	0.12	4.8	5.3

[a] CS = 0.05 μg/ml, MDH = 0.50 μg/ml

[b] CS = 0.05 μg/ml, MDH = 0.25 μg/ml

Figure 12. Rate constant of DTNB reaction in 34% PEG at 10°C. Reaction was monitored at 412 nm. CS concentration was kept at 0.5 µg/ml.

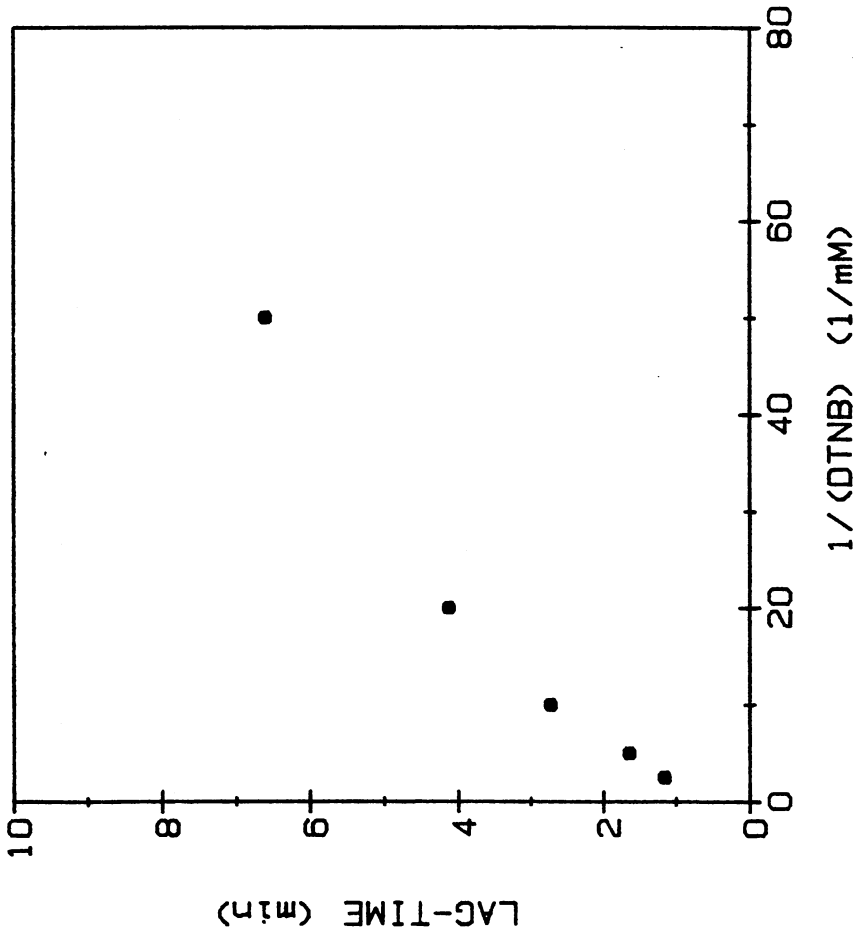
LAG-TIME (min)
0
2
4
6
8
10
0
20
40
60
80
1/(DTNB) (1/mM)

need not be linear. We measured the individual CS reaction rates with varying CS concentrations and measured the intrinsic lag-time due to the DTNB reaction (Table III). The results essentially show no variation of DTNB lag-time with CS concentration.

To ascertain that there is no hysteretic transition of the enzymes at the concentrations studied, normalized progress curves (normalized with respect to enzyme concentrations) were plotted (Figures 13 and 14). No anomalous behaviour was observed, evidenced by the superposition of the progress curves at different enzyme concentrations, for both MDH and CS.

Having shown that the soluble enzymes have nearly the expected lag-time, the measurements were repeated with solid-state enzymes. A much shorter lag time is observed (Figure 15) than the predicted 0.7 min (the K_{OAA} of solid-state CS was found to be 3.7 μM by least square fits to full progress curves, and V_1 was measured to be 5.0 μM M/min). The disappearance of the lag-time in the solid-state system indicates that OAA is directly channeled from MDH to CS.

Though the results looked very persuasive, further consideration, however, made these lag time results inconclusive because the predicted lag-time for solution-phase enzymes was only about 3 times the minimum observable reaction time. Systematic errors in determining the K_m and V_m might be of this magnitude considering the

TABLE III

LAG TIME DUE TO DTNB REACTION

DTNB = 400 μM

CS μg/ml	Lag Time min
1.00	1.42
0.75	0.80
0.50	1.16
0.25	1.58
0.10	1.26

Figure 13. Superimposed progress curves for MDH. MDH concentrations were 1.0 µg/ml (o), 6.0 µg/ml (●), and 10.0 µg/ml (x). The reactions were measured in the direction of malate oxidation, at 340 nm.

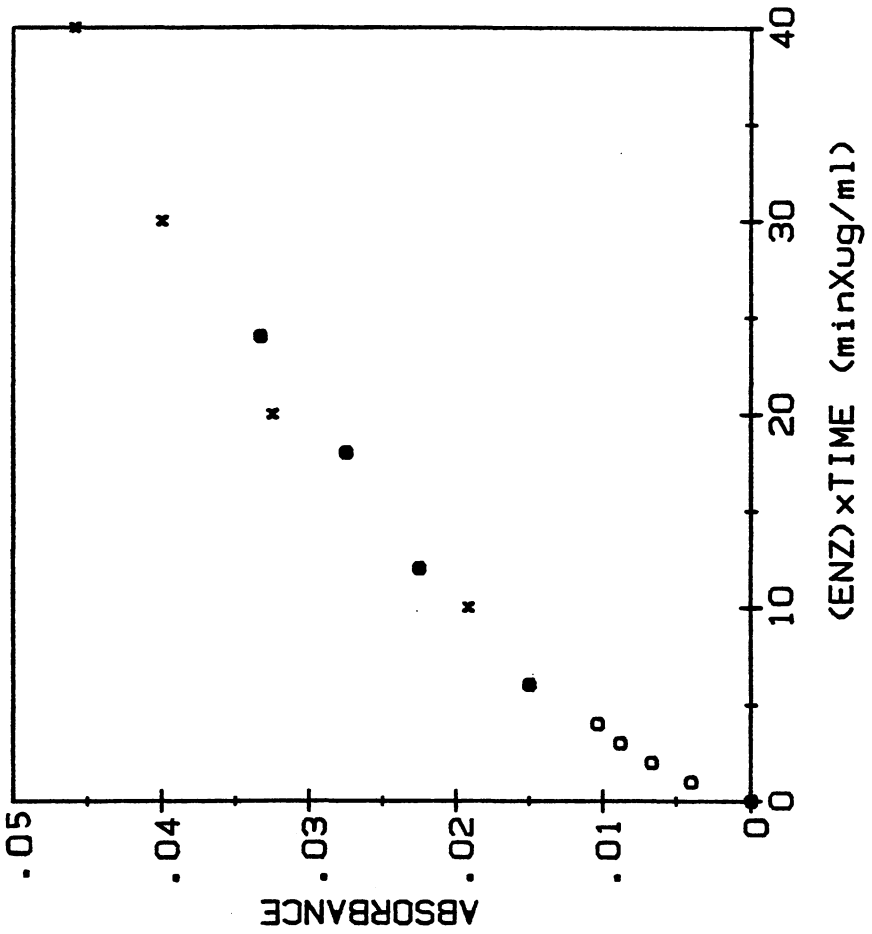
ABSORBANCE
.05
.04
.03
.02
.01
0
0
10
20
30
40
(ENZ)xTIME (minXug/ml)

Figure 14. Superimposed progress curves for CS. CS concentrations were 0.1 µg/ml (x), and 1.0 µg/ml (o). The reaction was monitored at 412 nm.

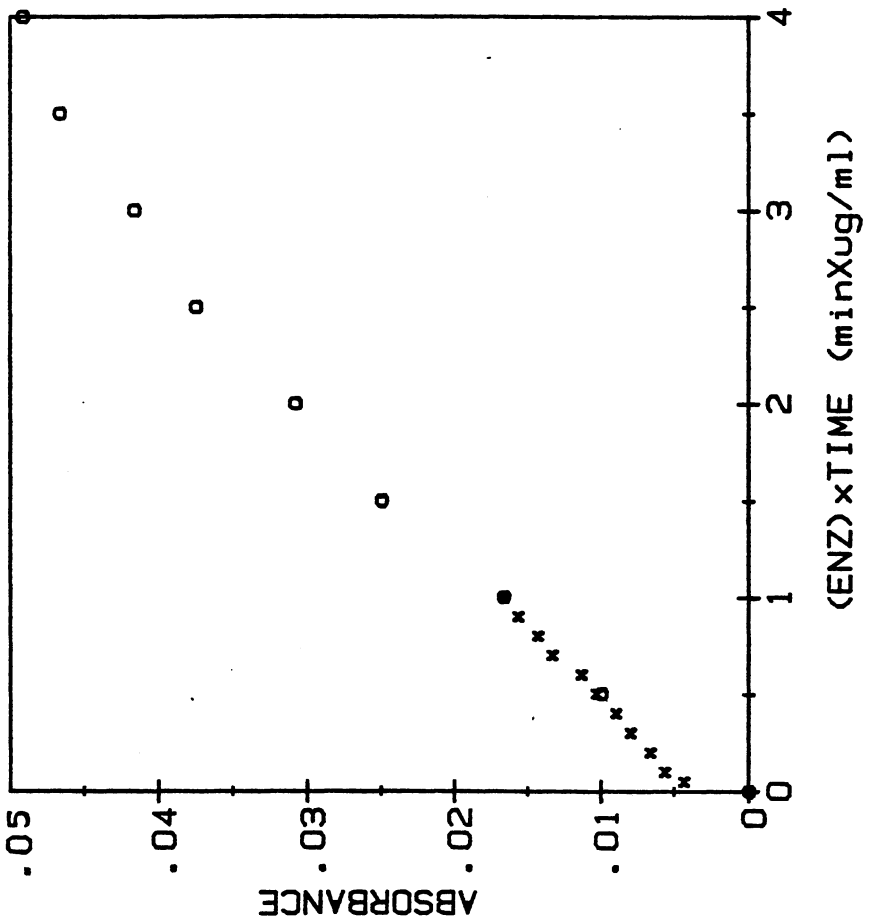
ABSORBANCE
.05
.04
.03
.02
.01
0
0
1
2
3
4
(ENZ)xTIME (minXug/ml)

Figure 15. Lag-time measurements with solid-state MC complex in 34% PEG at 10°C.

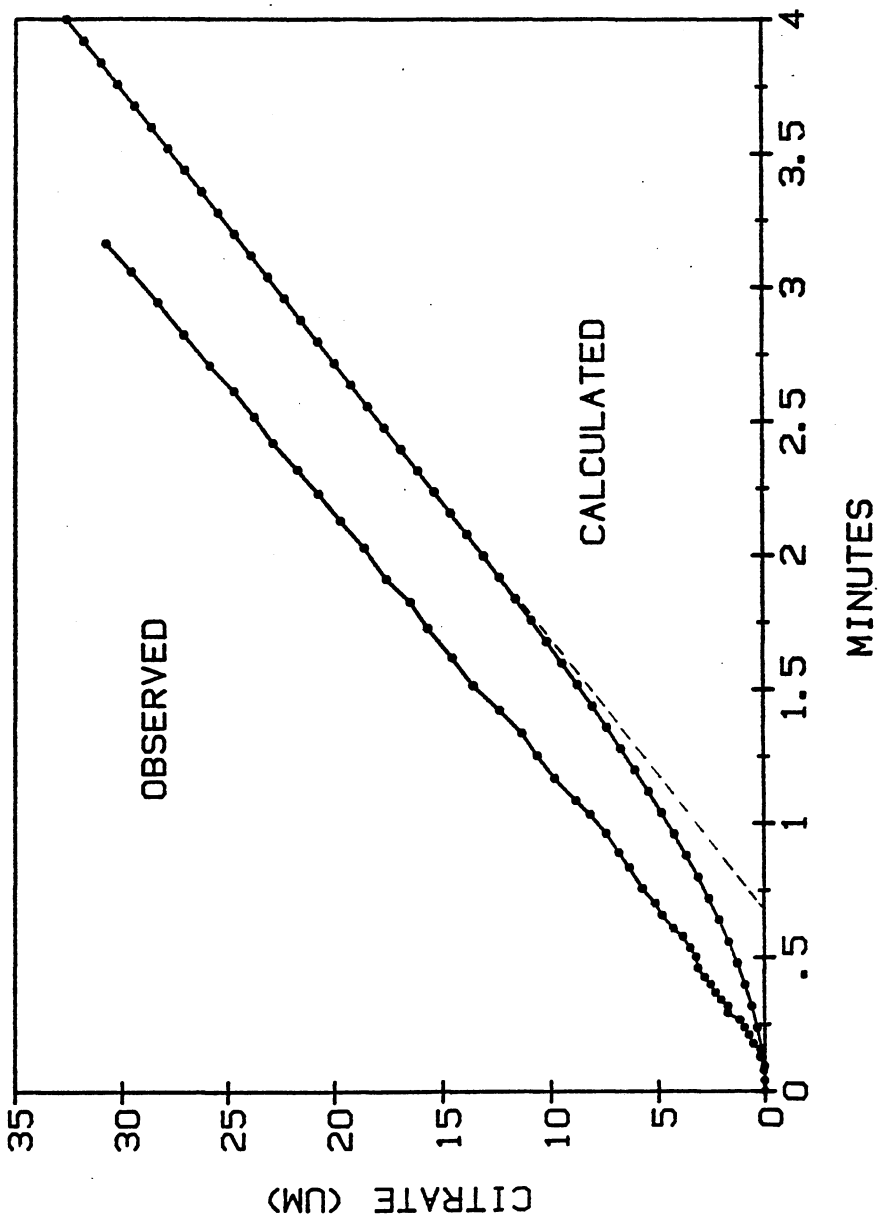
CITRATE (UM)
35
30
25
20
15
10
5
0
0
.5
1
1.5
2
2.5
3
3.5
4
MINUTES
OBSERVED
CALCULATED

experimental complications of this system. So the situation demanded further rigorous experimentation which would not require experimental kinetic constants and are much more sensitive in detecting substrate channeling.

"Trapping" Experiment

To provide a more accurate measure of substrate channeling, we developed an alternative method. In this method, any intermediate escaping from the vicinity of the coupling enzymes is trapped, thus reducing the rate of the coupled reactions. The trap is so effective that the coupled reaction rate is reduced to 1% or less of its control value should the intermediate be uniformly distributed in the bulk phase, as it must with unassociated solution-phase enzymes. In the case of the MDH-CS reactions studied here, the trap for OAA was AAT.

To test for escape of OAA from the solid-state enzymes into the solution phase, high concentrations of AAT with glutamate were used to trap solution phase OAA. The solubility of AAT in 34% PEG at 10^{o}C was determined in a separate experiment. We found, under the experimental conditions, approximately 88% of the enzyme is soluble at the maximum concentration we used (namely, 0.2 mg/ml), after one hour of incubation. So we can claim that the transferase was soluble in the reaction system, at least in the first few minutes of the reaction during which our measurements were over. (In our experience, turbidity of

precipitation requires several minutes to develop under similar conditions). The reaction was monitored by measuring the production of CoA at 412 nm. Our control contained everything except AAT. Table IV summarizes the results. It shows that the excess transferase trapped virtually all of the MDH-generated OAA when soluble phase MDH and CS were used. No detectable loss of OAA occurred, however, when solid-state enzyme complex was used. In summary, any OAA generated by MDH is uniformly distributed in the bulk medium with solution-phase enzymes. Thus, this OAA is trapped by the excess AAT and its reaction, thereby preventing any citrate production. In the solid-state complex, however, the OAA does not escape from the complex, and AAT cannot act on it. Thus, a normal citrate production is observed. The OAA trapping experiment was also performed with the solid-state enzymes incubated for 10 minutes before starting the coupled reaction. As mentioned before (Figure 10), we would expect the solid-state enzymes to dissolve prior to the reaction. Negligible synthase reaction was observed, in keeping with this prediction.

The following observations and calculations would help us understand the results and their implications. Dark-field microscopic observations on an aliquot from a suspension of solid-state enzyme complex in our laboratory indicate particle sizes of about 1 micron diameter interspersed with larger aggregates of these particles. Assuming partial specific volumes of protein within the

TABLE IV

TEST FOR SUBSTRATE CHANNELING USING AAT

Sample	Sp. Ac. of Soln. Phase U/mg	Sp. Ac. of Solid-Phase U/mg
No AAT	22 ± 2	5.5 ± 0.5
With AAT	1 ± 1	6.0 ± 0.5

Solution or solid-state experiments were with the same ratio of enzyme concs. in 34% PEG, 100mM K-phosphate buffer at pH 7.5 and 10 C. AAT when present, was at 2000 U/U of synthase. The standard deviations shown are calculated from triplicate measurements in each case.

solid-state of 0.75 ml/g, an one micron particle would contain about 10 million protein molecules. We find the molar ratio of CS to be about 0.6 in the solid-state. From this, it follows that the density of CS is about 8 mM in the solid-state. Considering that the equilibrium constant of the MDH reaction is approximately 10^{-5} - 10^{-4}, the maximal concentration of free OAA (unbound to protein) in the interstitial fluid of the solid-state aggregate would be about 5 μM. Thus, on the average, each OAA molecule would be surrounded by 1000 molecules of CS. Under these conditions, it is reasonable that most OAA molecules would be converted to citrate before escaping from the solid-state aggregate.

From the content of MDH and CS (33), and mitochondria (34) in rat liver, one can calculate that there should be about 3×10^4 of each of these enzyme molecules per mitochondrion. If these enzymes do associate into an immobolized aggregate *in vivo*, as suggested by several experiments (9, 13), the size and other features of this aggregate are likely to be much different from the solid-state particles used in the experiments of this report. Also enzyme specific activities *in vivo* may be greatly different from those in our experiments. Nevertheless, the ratio of CS molecules to free OAA molecules generated from the MDH should be similar in both systems. Thus, a high probability of substrate channeling of OAA, exists in mitochondria. Since a solid-state complex

of MDH-CS would only occupy a small fraction of the matrix volume, we would expect the Krebs cycle activity to be largely independent of the total OAA concentrations in the matrix. Also we would expect that less OAA has to be generated to sustain a high flux rate in the Krebs cycle with substrate channeling than otherwise. Similar conclusions might be applicable to other substrates. The physiological significance of substrate channeling, however, should be greatest for those substrates like OAA, whose low concentrations would otherwise limit the Krebs cycle flux.

The relative magnitude of solid-state and solution phase enzyme activities is of interest. It is not certain to what extent the measured specific activities with the solid-state enzymes are low due to diffusion limitations. The specific activities of the solid-state enzymes were generally 2 to 4-fold lower than corresponding activities in the solution phase whether the forward or reverse dehydrogenase reaction or the synthase activities were measured. There is about 2.5-fold drop in activity of the enzymes from room temperature to $10^{\circ}C$. The substrate concentrations (malate and NAD^{+}) were at least 80 times greater for the forward than the reverse dehydrogenase reaction, yet a similar ratio of specific activities (solid-state/solution-phase) was obtained (Table V). It shows that the ratios of the velocities of the two phases in the two directions (which is also the same as the ratio of specific activities, since the results are normalized with

TABLE V

VELOCITIES OF REACTIONS

v_f^{solid} [a]	v_f^{soln} [b]	R_f [c]	v_r^{solid} [d]	v_r^{soln} [e]	R_r [f]
0.45	1.72	0.26	2.25	10.5	0.21

[a] Denotes velocity of solid-state MDH in the MC complex in μM/min measured in the direction of malate oxidation in 34% PEG at 10°C.

[b] Denotes velocity of soluble MDH under same conditions as in a.

[c] $R_f = v_f^{solid} / v_f^{soln}$

[d] Denotes velocity of solid-state MDH in the MC complex in μM/min in the direction of OAA reduction in 34% PEG at 10°C.

[e] Denotes velocity of soluble MDH under same conditions as in d.

[f] $R_r = v_r^{solid} / v_r^{soln}$

respect to enzyme concentrations) are very close. This suggests that very little diffusion limitation exists. The fact that Lineweaver-Burk plots with varying OAA substrate were linear also supports this conclusion. To ascertain that we were dealing with true V_{max}'s, we measured the velocity of MDH reaction, both forward and reverse, at various substrate concentrations keeping the ratio of two substrates constant. The shape of the curve ensured us that we were truly in the V_{max} region. One such curve is shown in Figure 16.

It is more likely that enzymatic activities were confined to the surface of the particles as indicated by the following evidence. PEG would not be expected to be within the domain of the solid-state particles, since it acts to exclude these enzymes from its environment, as indicated by several experiments (9, 13). Thus enzyme molecules within and on the surface of the particles should be free of the extensive PEG inhibition (about 20-fold) found in the solution-phase. The specific activities observed for both enzymes, therefore, are about 1% of those expected for uninhibited enzyme in the solution phase. A monomolecular shell of these enzymes at the surface of a 1 μm diameter particle would contain 1% of the total enzyme, and therefore, could provide for the observed specific activities. The same two-fold ratio of activities (solution to solid-state) was observed with the MDH reaction whether the forward or reverse reaction was measured. Since the

Figure 16. V_{max} of solid-state MDH reaction in the direction of OAA reduction in 34% PEG at 10°C. OAA/NADH ratio was kept equal to 0.5.

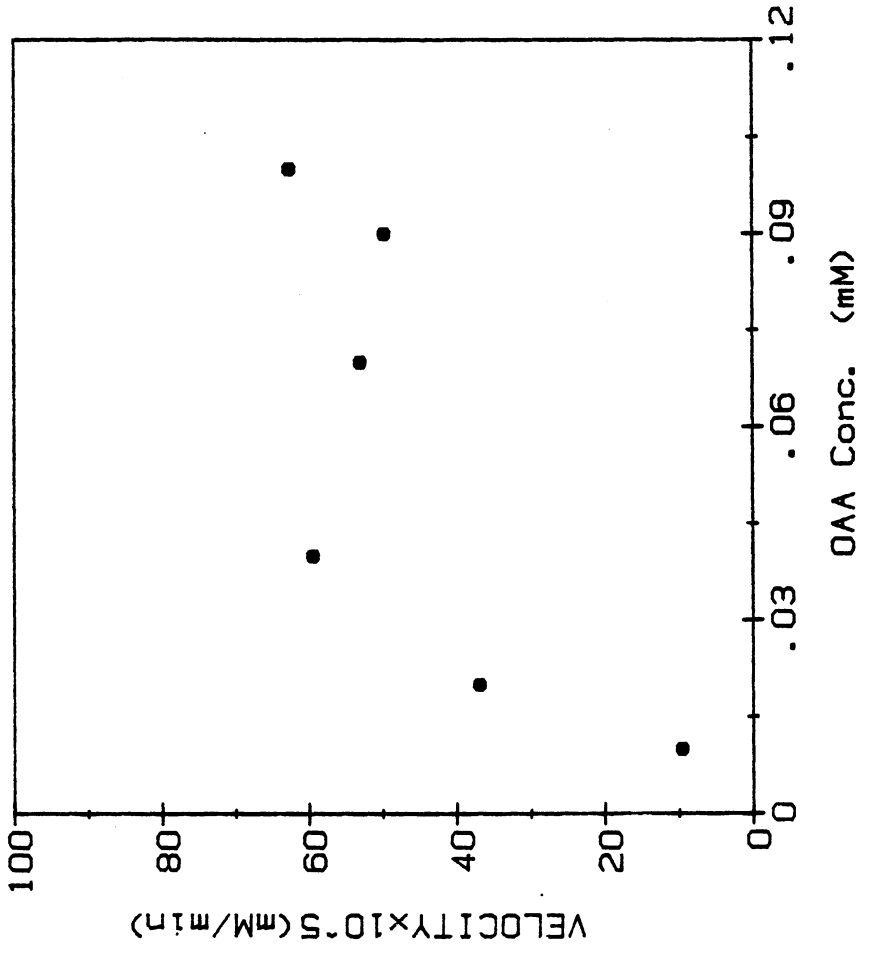
VELOCITY×10^5 (mM/min)
100
80
60
40
20
0
0
.03
.06
.09
.12
OAA Conc. (mM)

substrate concentrations are at least 80 times greater for malate oxidation, the lower specific activities in the solid-state are not likely due to a diffusion barrier. Secondly, molecular models of CoASAc indicate that it is too large to diffuse through close packed spheres of the size of the enzymes used (3).

Briefly, the outcome of our findings is that oxaloacetate is directly channeled from malate dehydrogenase to citrate synthase without escaping into the bulk medium. The possible physiological consequences of this finding are: (a) Krebs cycle activity could be independent of the total OAA concentration in the mitochondrial matrix. (b) Less OAA has to be generated to sustain a high flux rate in the Krebs cycle with substrate channeling than otherwise.

CHAPTER IV

SUMMARY AND CONCLUSIONS

There are reasons to believe that mitochondrial enzymes exist in closely associated forms. There are definite thermodynamic and kinetic advantages for the association of enzymes which are sequential in their reaction paths. In an *in vitro* system, we investigated two such enzymes, malate dehydrogenase and citrate synthase, which are adjacent to each other in the Krebs cycle. In this chapter I would like to summarize the results of our projects.

Solubility Profiles of MDH and CS

Our solubility data show that the solubility of MDH or CS, when present in combination with the other, decreases rapidly with increasing PEG concentration. When the enzymes are present alone, however, the solubility changes less rapidly with PEG concentration. Also, the solubility of both enzymes are decreased in the presence of the other as a result of coprecipitation. The solubility of MC complex increases with ionic strength and pH. The phenomenon is not ion-specific, since the same effects occur for both phosphate ions and chloride ions. Other experiments in our laboratory reveal the same profile for fluoride ions and

also for MOPS buffer. We chose to generate our solid-state MC complex in 10 mM potassium phosphate buffer (pH 7.5). Our solid-state MC suspension is a hetero-complex of MDH and CS in which less than 10% of the activity is contributed by solution phase enzymes. In this way we tried to mimic a physiological situation of solid-state enzymes in the mitochondrial matrix, as envisioned by Srere (2). Only a small fraction of the enzymes are associated in the solution phase, although the size of the associated complexes are enormous. This is because the solubility of the associated enzyme complexes is very low (35).

Kinetic Studies and Substrate Channeling

Conditions were found in which greater than 95% of the enzymes were in the solid-state. However, kinetic measurements could not be made at this solubility equlibrium. Therefore, kinetic measurements were made in an assay solution prior to solubilization of the MC complex. To achieve and demonstrate this conditions, an appropriate PEG concentration (34%) in the assay solution was found in which: (i) there were significant differences in the specific activities of the enzymes in the solid- and solution-states, and (ii) the rate of solubilization of the MC complex was sufficiently slow to permit kinetic measurements of the solid-state enzymes. Differences between the activities of solution- and solid-phase enzymes were used to indicate that the enzymes remained in the

solid-phase during the kinetic measurements. Filtration and centrifugation methods were tried and found too slow and unreliable for this purpose. We chose a PEG concentration of 34% for subsequent measurements, because at that concentration we were able to distinguish between two states of enzymes by their observable difference in specific activity (Figure 9). There is an approximately three-fold change in specific activity between the solid and solution states of the enzymes. The enzymes remained in the solid-state if the reaction was initiated with no preincubation.

Lag-time measurements of the coupled reactions in 34% PEG at 10^{o}C were made with soluble and solid-state enzymes. The soluble system served as the control. All the substrates and the chromophore DTNB were present in the reaction cuvette except the intermediate, OAA. With soluble system the observed lag-time agreed with the predicted value (Table II). With the solid-state system, however, a much shorter lag-time was observed compared to the calculated value assuming OAA would not be channeled. The results were consistent with substrate channeling, but not as convincing as desired due to the likelihood of experimental errors and small differences between the predicted and minimum observable lag-times.

To circumvent this problem, we took a different approach which would not involve the experimental kinetic constants. We used high concentrations of AAT with

glutamate to trap solution phase OAA. Excess AAT trapped all of MDH-generated OAA when solution phase enzymes were used (Table IV), but no detectable loss of OAA occurred when solid-state enzyme complex was used. When the MC complex was incubated for 10 minutes in 34% PEG (during which the enzymes dissolve) prior to adding AAT and malate to start the coupled reaction, all of the generated OAA was trapped in keeping with our prediction.

Considering the ratio of enzyme to OAA molecules within or at the surface of the solid-state particles ($\sim$1000), one would expect OAA to be converted to citrate within a few molecular distances of the site of OAA generation. Although the size of the aggregates and enzyme specific activities in vivo may be greatly different from those in our experiments, the ratio of CS molecules to free OAA molecules generated from the MDH reaction should be similar in both systems. Thus a high probability of substrate channeling exists in the mitochondria.

The specific activities of the solid-state enzymes were generally 2 to 4-fold lower than corresponding activities in the solution phase. A similar ratio of specific activities (solid-state/solution-phase) was obtained although the substrate concentrations (malate and NAD^+) were at least 80 times greater for the forward than the reverse dehydrogenase reaction. This, the good fit we obtained with the full-time progress curve data, and the linearity of the Lineweaver-Burk plots with varying OAA suggest that very

little diffusion limitation exists in our system.

Since a solid-state complex of MDH-CS would occupy a small fraction of the matrix volume, we would expect that the Krebs cycle rate can act independently of the bulk concentration of OAA in the mitochondrial matrix. Thus "OAA substrate limitation" of Krebs cycle activity may be circumvented by direct substrate channeling of oxaloacetate from malate dehydrogenase to citrate synthase.

A SELECTED BIBLIOGRAPHY

(1) Denton, R. M., and Pogson, C. I. (1976) Metabolic Regulation, Chapman and Hill.

(2) Srere, P. A. (1980) Trends in Biochem. Sci., 5, 120-121.

(3) Srere, P. A. (1981) Trends in Biochem. Sci., 6, 4-6.

(4) Fulton, A. B. (1982) Cell, 30, 345-347.

(5) Yoshida, A. (1966) J. Biol. Chem., 241, 4966-4976.

(6) Minton, A. P. (1983) Molec. Cell. Biochem., 55, 119-140.

(7) Bachman, L., and Johansson, G. (1976) FEBS Letters, 65, 39-43.

(8) Fahien, L. A., and Kmiotek, E. (1979) J. Biol. Chem., 254, 5983-5990.

(9) Halper, L.A., and Srere, P. A. (1977) Arch. Biochem. Biophys., 184, 529-534.

(10) Srere, P. A. (in press) Organized Multienzyme Systems: Catalytic Properties, G. R. Welch ed., Academic Press.

(11) Koch-Schmidt, A.-C., Mattiason, B., and Mosbach, K. (1977) Eur. J. Biochem., 81, 71-78.

(12) Srere, P. A., Mattiason, B., and Mosbach, K. (1973) Proc. Natl. Acad. Sci., 70, 2534-2538.

(13) Merz, J. M., Appleman, J. R., Webster, T. A., Taylor, T. W., Ackerson, B. J., Yu, H.-A., Ahern, J. A., Hague, J. W., and Spivey, H. O. (1981) Federation Proceedings, 39, 1630 (Abstract No. 153).

(14) Atha, D. H., and Ingham, K. C. (1981) J. Biol. Chem., 256, 12108-12117.

(15) Gaertner, F. H., Ericson, M. C., and DeMoss, J. A. (1970) J. Biol. Chem., 245, 595-600.

(16) Bryce, C. F., Williams, D. C., John, R. A., and Fasella, P. (1976) Biochem. J., 153, 571-577.

(17) Sumegi, B., and Alkonyi, I. (1983) Biochim. Biophys. Acta, 749, 163-171.

(18) Porpaczy, Z., Sumegi, B., and Alkonyi, I. (1983) Biochim. Biophys. Acta, 749, 172-179.

(19) Lehninger, A. L. (1946) J. Biol. Chem., 164, 291-306.

(20) Lopes-Cardozo, M., and Van den Bergh, S. G. (1972) Biochim. Biophys. Acta, 283, 1-15.

(21) Williamson, J. R., Scholz, R., and Browning, E. T. (1969) J. Biol. Chem., 244, 4617-4627.

(22) Srere, P. A. (1972) Energy Metabolism and the Regulation of Metabolic Processes in Mitochondria, M. Mehlman, and R. W. Hanson eds., Academic Press, New York, 79-91.

(23) Christopherson, R. I., Jones, M. E., and Finch, L. R. (1979) Anal. Biochem., 100, 184-187.

(24) Singh, M., Brooks, G. C., and Srere, P. A. (1970) J. Biol. Chem., 245, 4636-4640.

(25) Thorne, C. J. R. (1962) Biochim. Biophys. Acta, 59, 624-633.

(26) Srere, P. A. (1969) Meth. Enzymol., 13, 5.

(27) Williamson, J. R., and Corkey, B. E. (1969) Meth. Enzymol., 13, 468-470.

(28) Nisonoff, A., and Barnes, F. W., Jr. (1952) J. Biol. Chem., 199, 713-728.

(29) Hill, D. E., and Spivey, H. O. (1974) Anal. Biochem., 57, 500-505.

(30) Chandler, J. P., Hill, D. E., and Spivey, H. O. (1972) Comput. Biomed. Res., 5, 515-534.

(31) Manley, E. R., Webster, T. A., and Spivey, H. O. (1980) Arch. Biochem. Biophys., 205, 380-387.

(32) Davis, L. C., Cate, R. L., and Roche, T. E. (1979) Anal. Biochem., 97, 428-437.

(33) Srere, P. A. (1967) Science, 158, 936-937.

(34) Reith, A., Barnard, T., and Rohr, H.-P. (1976) CRC Critical Reviews in Toxicology, 4, 219-269.

(35) Appleman, J. R. "Effect of Polymers on Physical and Kinetic Properties of Glutamate Dehydrogenase from Bovine Liver." (Unpublished Ph.D. thesis, Oklahoma State University, 1983.)

PART TWO

POLYETHYLENE GLYCOL INDUCED PROTEIN ASSOCIATIONS

CHAPTER I

INTRODUCTION

Interaction betwen proteins and polymers has been the focus of attention of many scientists for a variety of reasons, including protein purification, crystallization and understanding the state of aggregation of proteins in an *in vivo* system where they are present with different organic macromolecules. For years synthetic polymer polyethylene glycol (PEG) has been used to study this type of interactions, not only with proteins but with other macromolecules also. In this respect, it has wide variety of applications in chemical and biomedical industries also. The effects of PEG on macromolecular solutions can be classified into four different groups: (a) precipitation (1), association, either a self-association of macromolecules or association of macromolecules with other macromolecular components (2), (c) contraction in size of macromolecules (3), and (d) it can cause the macromolecules to pass into a second aqueous phase (4). These effects probably have a common cause in the excluded volume property of PEG (5,6), although alternative explanations (7,8) have been given.

According to the widely accepted excluded volume

theory, proteins are sterically excluded from regions of the solvent occupied by inert synthetic polymers causing a large negative entropy of mixing of the polymer with the protein. Thus, addition of the polymer which has associated with it the excluded volume increases the free energy of the system by virtue of decreasing the entropy. There are four possibilities that can minimize this unfavourable free energy change. First, the protein and polymer can phase separate into two aqueous phases; secondly, they can separate into a precipitated and a solution phase; thirdly, both the macromolecules can undergo a conformational change, and fourthly, the macromolecules can self-associate. All of these effects can minimize the excluded volume effect of one on the other. The effects of the association of the macromolecules and the conformational change result in a more compact spherical formation of the macromolecules. Each of these actually reduces the interaction between the soluble polymer and the macromolecule and thereby reduces the unfavourable free energy. Another group of workers (7,8) considers protein surfaces covered by a mosaic of charges. At such an interface the interaction of PEG and these charges is thermodynamically unfavourable leading to exclusion of PEG from the protein domain.

There are reasons why PEG would be expected to provide such large excluded volume effects. These reasons are: (i) high water solubility of PEG, (ii) its extended conformation, (iii) its low molecular weight while still

being a macromolecule; this provides a large molar concentration at a low weight concentration. Minton's theory (5) shows that the effect at a given weight per cent of polymer is inversely proportional to the molecular weight. In other words, excluded volume effect at a given weight per cent increases with decreasing molecular weight of the macromolecule. In the realm of macromolecules that exclude a significant volume fraction, this inverse relationship between the magnitude of excluded volume effect and the molecular weight holds very rigorously. Also, the magnitude of the driving force is a function of polymer concentration and the molecular size of the polymer (7).

The following virtues of PEG make it a good polymer to study the polymer-protein interactions. (i) It is an unbranched polymer with no ionic groups. This simple structure of PEG makes interpretation of polymer-protein effects easier. (ii) It is highly soluble in water. (iii) It is non-denaturing. Proteins remain quite stable for a long period of time in presence of high concentrations of PEG.

Rationale and Objectives

For a number of years our laboratory has been engaged in the characterization of PEG induced association of MDH and CS. Halper and Srere (9) were the first to demonstrate that mitochondrial MDH and CS interact in presence of PEG and that the interaction is very specific. But their study

did not reveal anything about the association of the enzyme in solution phase. They only investigated coprecipitation. Subsequent to this observation, our laboratory (10) has shown that PEG induces the association for each of the enzymes alone and to a greater extent for the mixture. The association was found to occur to extremely large molecular weight aggregates, approaching one micron in diameter. This association is undetectable by most methods, because more than 99% of the mass of the enzymes remained as monomers. Dynamic light scattering (DLS) method is able to detect this type of association, because the intensity of the signal is proportional to the second moment of the molecular weight distribution. We will discuss the principle of this mehod in more detail in the following chapter.

Having found this type of association between MDH and CS in each of the cases, the enzymes alone and their mixture, we suspected that it may be a general phenomenon and thus chose five additional proteins to investigate, covering a wide molecular weight range from 14.4 to 670.

Although excellent agreement between excluded volume theory and the results from equilibrium dialysis and light scattering data on PEG and protein solutions exists, discrepancies with protein solubility data are very large (10). Knoll and Hermans (11) argued that the discrepancy is due to the penetration of lower molecular weight polymers into the protein-rich phase. Data (10,11) testing this view are contradictory. Results presented in this thesis should

provide another explanation for the discrepancy between the excluded volume theory and solubility data. We will discuss them in Chapter III.

CHAPTER II

EXPERIMENTAL

Materials

Fibrinogen and bovine chymotrypsin were purchased from Calbiochem and the rest of the proteins were from Sigma. Screw cap glass vials of 3.5 ml capacity, used for light scattering measurements were purchased from Pierce Chemical Company. PEG 6000 was from Matheson Coleman and Bell. Light scattering measurements were made at 22^{o}C in 0.05M potassium phosphate buffer (pH 7.0), containing 0.1M KCl. PEG solutions were also made in the same buffer. The solubility of all the proteins under these conditions were previously determined by incubating the proteins in PEG solutions for an hour followed by centrifugation at 10,000g for 40 minutes. Protein contents in the supernatants were determined spectrophotometrically. Specific absorptivity values of 2.6, 2.04, 0.91, 1.55, and 1.04 $(mg/ml)^{-1}cm^{-1}$ were used for lysozyme, chymotrypsin, aldolase, fibrinogen and thyroglobulin, respectively (12).

Methods

Dynamic Light Scattering

Theory. The method involves the measurement of scattered light intensities from a small volume of sample illuminated with laser beam. The molecules within this volume element undergo Brownian motions. This type of random motion creates a fluctuation in the scattered intensity which can be directly related to the diffusion coefficients, D, of the macromolecules. Small molecules diffuse more rapidly than the larger ones. The intensity due to these diffusive motions is sampled and stored in 64 different memory locations ("channels") of the computer. Sample times can be 1 μsec and up.

The relationship to D is obtained from the correlation function (13). The correlation function of two signals is obtained by evaluating the time averaged or integrated product of the two signals as a function of their relative displacement on a time scale. If two signals are the same, autocorrelation function is obtained by application of the following equation

$$G^{(2)}(\tau) = \lim_{T\to\infty} (1/T)\int_0^T I(t)\,I(t+\tau)\,dt$$

where τ is the correlation time and T is the total time. Correlation time is directly identifiable with the sampling time. To illustrate the process of correlation, let us consider the autocorrelation of a sine wave. First, the sine wave is multiplied in phase, i.e., $\tau = 0^{\circ}$. The result

is a $\sin^2$ wave. To complete the evaluation of the autocorrelation function at this relative displacement, the average value of $\sin^2$ wave must be determined. Similarly, the autocorrelation functions at τ values of 90°, 180°, and 270° can be determined. The resulting function will be a cosine wave. To compute the autocorrelation functions of nonperiodic or random (noise) waveforms, one has to recognize that any wave, whether periodic or not, is composed of sine wave components. When many such components are present in a parent waveform, the resulting autocorrelation will be the sum of the autocorrelation functions of the components. The random noise is the result of the Brownian motion of finite size molecules. That is, the high frequency components of I are limited by the size of the molecule. Precise mathematical analysis of the autocorrelation function, $g(\tau)$ shows that it is a single exponential decay function for random signals corresponding to the Brownian motion of a single molecular component. The decay constant of g is a simple function of the different coefficients of the component defined below. Intuitively, then one can understand how the autocorrelation function is related to D, the diffusion coefficient. For larger molecules, the random motions are slower (lower D) and the delay time must, therefore, be larger before the two signals become "uncorrelated". Thus, the g function for larger molecules decays more slowly. The correlation function from a mixture of independent macromolecules is the sum of

exponential functions characterizing the macromolecules alone. Spatial fluctuations, as specified by the wave number K of the fluctuation responsible for the scattering, is defined as

$$K = \{4\pi n \sin(\theta/2)\}/\lambda \qquad (2\text{-}1)$$

where n = the refractive index of the medium

λ = the wavelength of light

θ = the measuring angle of the detector.

For monodisperse systems the heterodyne or cross-correlation function $g^{(1)}(\tau)$ is related to the diffusion coefficient, D, by $g^{(1)}(\tau) = Ae^{-\Gamma\tau}$ where $\Gamma = DK^2$, and for paucidisperse systems, $g^{(1)}(\tau) = \Sigma A_i e^{-\Gamma_i \tau}$. The cross-correlation function is similar to the auto-correlation function. In the former case, the light scattering from the solute is correlated with the incident light rather than with a copy of the solute-scattered light.

The diffusion coefficient is related to the viscosity of the medium and the particle radius in the following way

$$D = k_B T_A / 6\pi\eta a \qquad (2\text{-}2)$$

where k_B = the Boltzmann constant

T_A = the temperature (degrees Kelvin)

η = the viscosity of the medium

a = the particle radius.

For wide molecular weight distributions, the following averaging functions (moments) of the correlation functions are often cited:

The average time constant $T = \Sigma A_i T_i / \Sigma A_i$ (2-3)

where $T_i = 1/\Gamma_i$. T is calculated as the area under the normalized autocorrelation curve using a computer program written by Jim Appleman.

The average decay rate $\Gamma = K_1 = \Sigma A_i \Gamma_i / \Sigma A_i$ (2-4)

where K_1 is the first cumulant(14).

Using equations (2-1), (2-2), (2-3), and (2-4) it is possible to get an estimate of the average diffusion coefficients of the particles, and hence their apparent molecular weights and particle radii.

The apparent z-average molecular weights of the particles are calculated using the following formula:

$$M_p = (a_p^3/a_m^3) M_m$$

where M_p = apparent z-average molecular weight of the associated particle

a_p = z-average radius of the associated particle

a_m = radius of the unassociated particle

and M_m = molecular weight of the monomer.

To fully appreciate the advantages of DLS method, we have to remember that the extent of protein asociation induced by PEG in terms of size is astronomical; but the extent of association in terms of the fraction of mass is extremely small. Less than one per cent of the total mass is involved in association. The advantage of DLS is that its signal is proportional to the square of the molecular weight and hence the contribution from the associated species is often larger than the contribution from the 99% of the rest of the mass. Figure 1 represents an example of

Figure 1. Normalized cross correlation functions of MDH-CS system. (o) Without PEG, (x) with PEG. g stands for the normalized correlation function.

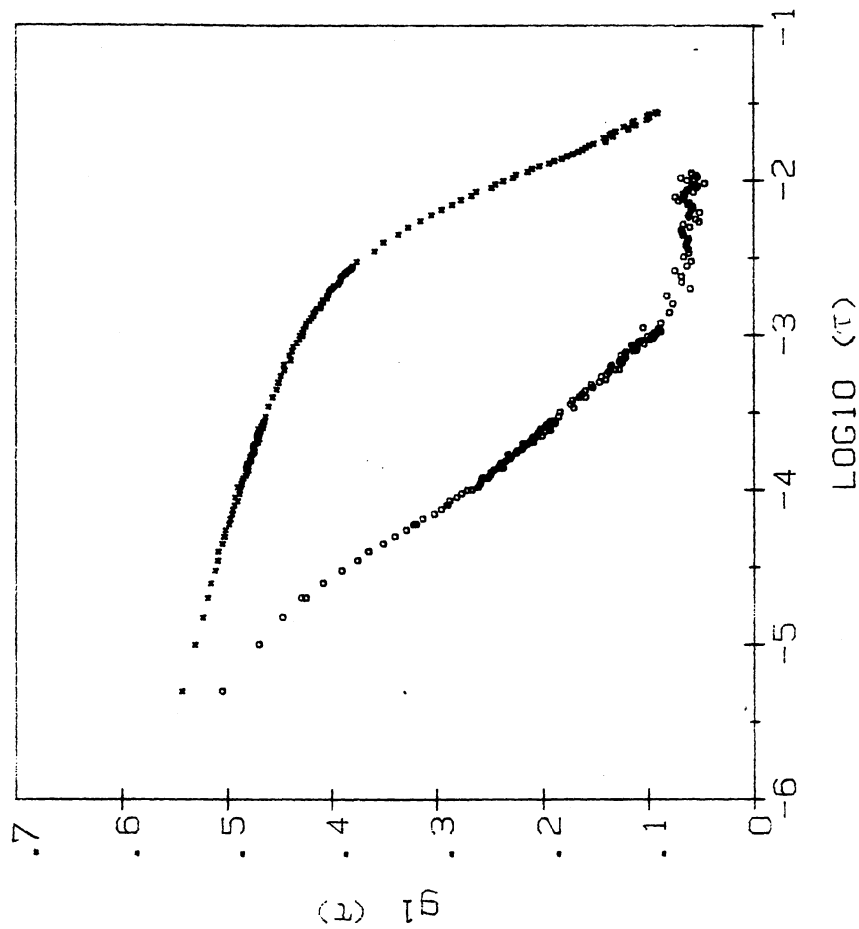
.7
.6
.5
.4
.3
.2
.1
0
-6
-5
-4
-3
-2
-1
LOG10 (τ)
g1 (τ)

correlation functions with MDH-CS system obtained in our laboratory. When there is no PEG the correlation curve decays very quickly with an exponential deacy rate; but in presence of PEG it approaches the baseline much more slowly, at a longer sampling time and the exponentiality is lost showing the presence of high molecular weight agreegates.

Experimental. The prime requirement for light scattering measuremnts is that all the samples and vials be free of contaminating light scattering sources ("dust" particles or scattering imperfections in the glass). The following precautions were adopted to make the samples dust-free. Buffers and PEG solutions were filtered through pre-wetted Milex-GV 0.22 µm disposable filter units. Stock protein solutions were first centrifuged at 10,000g for an hour to get rid of large particles and subsequently pipetted into the vials using cleaned disposable pipet tips. Vials and pipet tips were cleaned with deionized water followed by deionized water passed through Milex-GV 0.22 µm filter units.

Light scattering of the samples was monitored at 90^{o} using an ITT FW photomultiplier. The light source was a laser beam. The wavelengths used were 514.8 nm and 632.8 nm, for two different sources used. The autocorrelation function of the scattering intensity was calculated by a Langley-Ford autocorrelator interfaced to a PDP 11/10 minicomputer. The data were stored on flexible disks for later analysis on a PDP 11/40 minicomputer. Calculated

diffusion coefficients were corrected for the viscosity of the medium. Viscosities of different PEG solutions were determined at 22^{o}C, using Ostwald glass viscometer. For different values of viscosities at different PEG concentrations, see the table under Results and Discussion. Intensity values were normalized with respect to that of standard latex solutions. The refractive index n was taken as 1.33.

CHAPTER III

RESULTS AND DISCUSSION

Suitable protein and PEG concentrations were first sought to give substantial protein associations, yet remain far from protein solubility limits. Protein solubility was determined by the method as described in Chapter II. Table I gives the solubility of the proteins and actual protein and PEG concentrations used in the experiment. It also shows the viscosity of different PEG solutions which we used in calculating the diffusion coefficients later.

Table II shows the scattered intensities of the beam when the proteins are in buffer or in PEG solutions. The scattered intensity of the sample was normalized with respect to previously calibrated turbidity of standard latex solutions by static light scattering measurements. Our results show that there is several fold increase in scattered intensity when the proteins are in PEG solution than when they are present in buffer. The increase in scattering intensity cannot be attributed to the presence of PEG *per se*, because the maximum time at which the correlation due to PEG alone was observed was found to be of same order of magnitude or less as that for proteins in buffer (less than 10 μsec; data not shown). Decay of the

TABLE I

SOLUBILITY OF THE PROTEINS IN PEG SOLUTIONS

Protein	PEG Conc. %	Solu. mg/ml	Prot.Conc. Used mg/ml	Viscosity of PEG cp
Lysozyme	20	4.2	2.5	14.1
Chymotrypsin	5	10.3	5.0	2.2
Aldolase	12	3.5	1.5	5.7
Fibrinogen	2	2.3	1.5	1.3
Thyroglobulin	8	14.7	7.0	3.3

TABLE II

SCATTERING INTENSITY OF PROTEINS

Protein	Intensity in absence of PEG	Intensity in presence of PEG	Ratio of Intensities
Lysozyme	0.00011	0.0041	36.4
Chymotrypsin	0.00050	0.0015	3.0
Aldolase	0.00032	0.0024	7.5
Fibrinogen	0.00130	0.0040	3.1
Thyroglobulin	0.00160	0.0255	15.9

correlation function of proteins in buffer was complete before those of the associated particles began. Data in the last eight channels always approached the theoretical baseline to within 1% or less.

The diffusion coefficients of the proteins in buffer without PEG, calculated from the single exponential fit of the correlation curve, agreed well with the published values (Table III) with the exception of chymotrypsin and aldolase. For chymotrypsin, no single value was found. This is probably due to its self-association, the extent of which depends on the ionic strength of the solution (14,15). For aldolase, the little discrepancy might be due to the presence of slight amount of denatured materials in the sample, although differences in sedimentation coefficients and molecular weights in different laboratories with no plausible reason were previously reported (16).

Table IV summarizes the diffusion coefficients and molecular weights of the associated proteins using both of the well defined Γ averages (those obtained from: (a) average decay rate Γ, and (b) average time constant T). In the first method, the average diffusion coefficient, D_{av1}, was calculated using the equation $D_{av1} = K_1/K^2$, where K_1 is the first cumulant, calculated by computer fit, and K is defined in equation (2-1). In the second method, the average diffusion coefficient, D_{av2}, was calculated using the equation $D_{av2} = 1/(TK^2)$ assuming the decay is exponential, where the average time constant, T, was

TABLE III

DIFFUSION COEFFICIENTS IN ABSENCE OF PEG

Protein	$10^7 \times D^{obs}$ cm^2/s	$10^7 \times D^{pub}$ cm^2/s
Lysozyme	11.7	10.4 (18)
Chymotrypsin	0.24	--[a]
Aldolase	2.8	4.4 (16)
Fibrinogen	1.8	2.0 (19)
Thyroglobulin	1.9	2.4 (20)

[a] No single published value was found (see Text)

TABLE IV

DIFFUSION COEFFICIENTS AND MOLECULAR WEIGHTS IN PRESENCE OF PEG

Protein	10^{-3} x MW of monomer	10^{10} x D cm^2/s	10^{-3} x M_p/M_m
Chymotrypsin[a]	24.5	1.8	2.3×10^6
Lysozyme[a]	14.4	5.7	3.1×10^3
Fibrinogen[b]	340	1×10^2	1×10^3
Aldolase[b]	149	4.3×10^2	2.0
Thyroglobulin[b]	670	5.8×10^3	1.1×10^{-3}

[a]Average diffusion coefficient calculated by cumulant method.

[b]Average diffusion coefficient calculated from integrated time constant.

calculated from the area under the normalized autocorrelation curve. The apparent molecular weights of the associated proteins were computed using equation (2-2) and (2-3). When data were collected at a long sampling time the second method was applied, which would give a minimum estimate of the molecular weight of the associated protein. The integrated time constant was divided by 1 to normalize for the amplitude. For data at shorter sampling times, cumulant method was applied. From the average values of diffusion coefficients and the ratio of molecular weights (M_p/M_m), we see an astronomical increase in average molecular weights of the proteins with a concommitant decrease in their diffusion coefficient values. However, it is suspected that the low value of M_p/M_m for thyroglobulin is due to some noise present in the data for the protein in PEG. These dramatic changes in these values clearly imply an extensive protein self-association in terms of large molecular weight aggregates in presence of PEG.

Partial denaturation of the proteins by the PEG or contaminants within the PEG could also cause the light scattering results described above due to denatured protein aggregation. Several arguments exist against denaturation and for PEG induced protein association, based on experiments with the MDH-CS-PEG system as follows. Recrystallization of PEG, which removes ultraviolet absorbing contaminants, does not reduce the PEG induced association of MDH, CS, or the enzyme mixture (unpublished

results, our laboratory). PEG dramatically enhances the stability of both MDH and CS under conditions of the DLS measurements. It is still conceivable that a low level contaminant in the PEG might denature a stoichiometric equivalent amount of protein, while the remaining protein is stabilized by the PEG. The most persuasive evidence against this is that the size of the associated MDH-CS particles in the presence of PEG is considerably greater than the particle sizes with either enzyme alone, that is, the addition of, for example, MDH to a CS-PEG mixture causes considerable increased particle sizes (presumably due to formation of MDH-CS complexes) though the PEG concentration is not changed. No increased particle sizes are observed when MDH is added to CS without PEG. We do not think these observations are compatible with protein denaturation caused by PEG sample. This latter evidence, based on hetero-associations, is not possible to gather on the self-associations of the other proteins. The sum of the above evidence and the similarity of the light scattering effects among all the proteins examined, however, indicate that the same mechanism is operating in each case.

In Chapter I it was mentioned that discrepancy between excluded volume theory and solubility data exists. Results presented in this thesis provide another explanation for this discrepancy. The results indicate that PEG causes all proteins to associate into extremely high molecular weight aggregates which are the insoluble species. The theory

based on the solubility data presumes that the insoluble species is the monomer which has a much smaller molecular volume. Calculations from the solubility data indicate a protein excluded volume which is many times larger than is understandable if it is viewed as the monomeric enzyme, in keeping with our argument.

CHAPTER IV

SUMMARY AND CONCLUSIONS

The purpose of this study was to investigate the generality of the protein-associating effect of PEG. Five proteins with a wide range of molecular weights were chosen and the DLS method was utilized to detect and physically characterize the association. DLS proved to be a very sensitive technique to detect this type of association where the extent of association in terms of mass is very small, although in terms of size it is astronomical.

Solubility of each of the proteins in PEG solutions was determined previously. Protein and PEG concentrations were chosen suitably so that a convenient working protein concentration can be used, still being far below its solubility limit. Several fold increase in scattered intensity was found when the proteins were present in PEG, compared to buffer. The enhancement in scattering intensity could not be attributed to the presence of PEG *per se* and was concluded due to the self-association of the proteins in presence of PEG. Diffusion coefficients of the proteins in buffer without PEG were calculated using the single exponential fit of the correlation functions and in most cases the results agreed well with the published values.

Diffusion coefficients of the proteins in presence of PEG were calculated by two methods, one from the first cumulant, the other using the average time constant. Table II indicates an extensive self-association of the proteins in terms of large molecular weight aggregates in presence of PEG evidenced by a considerable decrease in average diffusion coefficients and a significant increase in the average molecular weights of the proteins in presence of PEG. All these evidence point to the fact that the proteins tested underwent an extensive self-association to large molecular weight aggregates in presence of PEG.

Partial denaturation of the proteins resulting in increased light scattering was ruled out by our observations with MDH-CS-PEG system where PEG dramatically enhanced the stability of the enzymes under conditions of DLS measurements.

So our conclusion was that PEG causes all proteins to associate into extremely high molecular weight aggregates which are insoluble species. These findings offer an alternative explanation for the discrepancy between excluded volume theory and solubility data, by showing that, unlike the assumptions in solubility data, the insoluble species are highly associated enzymes having a large molecular volume.

A SELECTED BIBLIOGRAPHY

(1) Jukes, I. R. M. (1971) Biochim. Biophys. Acta, 229, 535-546.

(2) Herzog, W., and Weber, K. (1978) Eur. J. Biochem., 91, 249-254.

(3) Lerman, L. S. (1971) Proc. Natl. Acad. Sci. USA, 68, 1886-1890.

(4) Albertsson, P. A. (1971) Partition of Cell Particles and Macromolecules, 2nd ed., Almqvist and Wiksell, Stockholm and Wiley, New York.

(5) Minton, A. P. (1983) Molec. Cell. Biochem., 55, 119-140.

(6) Hermans, J. (1982) J. Chem. Phys., 79, 2193-2203.

(7) Lee, J. C., and Lee, L. L. (1981) J. Biol. Chem., 256, 625-631.

(8) Timasheff, S. N., Lee, J. C., Pittz, E. P., and Tweedy, N, (1976) J. Colloid Interface Sci., 55, 658-663.

(9) Halper, L. A., and Srere, P. A. (1977) Arch. Biochem. Biophys., 184, 529-534.

(10) Merz, J. M., Appleman, J. R., Webster, T. A., Taylor, T. W., Ackerson, B. J., Yu, H.-A, Ahern, J. A., Hague, J. W., and Spivey, H. O. (1981) Federation Proceedings, 39, 1630 (Abstract No. 153).

(11) Knoll, D., and Hermans, J. (1983) J. Biol. Chem., 258, 5710-5715.

(12) Atha, D. H., and Ingham, K. C. (1981) J. Biol. Chem., 256, 12108-12117.

(13) Betty, K. R., and Horlick, G. (1976) Anal. Chem., 48, 1899-1904.

(14) Koppel, D. E. (1972) J. Chem. Phys., 57, 4814-4820.

(15) Pandit, M. W., and Rao, M. S. N. (1975) Biochemistry, 14, 4106-4110.

(16) Tellam, R., and Winzor, D. J. (1977) Biochem. J., 161, 687-694.

(17) Taylor, J. F., and Lowry, C. (1956) Biochim. Biophys. Acta, 20, 109-117.

(18) Sophianopoulos, A. J., Rhodes, C. K., Holcomb, D. N., and Van Holde, K. E. (1962) J. Biol. Chem., 237, 1107-1112.

(19) Putnam, F. W. (1975) The Plasma Proteins, Putnam, F. W. ed., Vol I, 57-131, Academic Press, New York.

(20) Edelhoch, H. (1960) J. Biol. Chem., 235, 1326-1334.

VITA

Asit Datta

Candidate for the Degree of

Doctor of Philosophy

Thesis: I. SUBSTRATE CHANNELING AND RELATED PROPERTIES OF THE MALATE DEHYDROGENASE-CITRATE SYNTHASE COMPLEX
II. POLYETHYLENE GLYCOL INDUCED PROTEIN ASSOCIATIONS

Major Field: Biochemistry

Biographical:

Personal Data: Born in Calcutta, India, October 4, 1954, the son of Amal K. and Roma Dutt. Married to Jhuma Dutt on June 26, 1981.

Education: Graduated from Hare School, Calcutta, India, in 1971; received the Bachelor of Science Degree in Physics from Presidency College (University of Calcutta), Calcutta, India, in 1974; received the Master of Science Degree in Physics from University of Calcutta, Calcutta, India, in 1976; completed requirements for the Doctor of Philosophy Degree at Oklahoma State University on December, 1984.

Professional Experience: Research Fellow, Department of Biophysics, Chittaranjan National Cancer Research Centre, Calcutta, India, from 1978 to 1980; Research Assistant, Department of Molecular Biology and Microbiology, Tufts University School of Medicine, Boston, Massachusetts, from January 1981 to December 1981; Research Assistant, Department of Biochemistry, Oklahoma State University, from January 1982 to December 1984.

Honorary Societies: Sigma Xi, Phi Lambda Upsilon.